

<https://helda.helsinki.fi>

Discovery of substituted oxadiazoles as a novel scaffold for DNA gyrase inhibitors

Jakopin, Ziga

2017-04-21

Jakopin , Z , Ilas , J , Barancokova , M , Brvar , M , Tammela , P , Dolenc , M S , Tomasic , T & Kikelj , D 2017 , ' Discovery of substituted oxadiazoles as a novel scaffold for DNA gyrase inhibitors ' , European Journal of Medicinal Chemistry , vol. 130 , pp. 171-184 . <https://doi.org/10.1016/j.ejmech.2017>

<http://hdl.handle.net/10138/301097>

<https://doi.org/10.1016/j.ejmech.2017.02.046>

Downloaded from Helda, University of Helsinki institutional repository.

This is an electronic reprint of the original article.

This reprint may differ from the original in pagination and typographic detail.

Please cite the original version.

Discovery of substituted oxadiazoles as a novel scaffold for DNA gyrase inhibitors

Žiga Jakopin^{a,}, Janez Ilaš,^a Michaela Barančoková,^a Matjaž Brvar,^b Päivi Tammela,^c Marija Sollner Dolenc,^a Tihomir Tomašič^a and Danijel Kikelj^a*

^aUniversity of Ljubljana, Faculty of Pharmacy, Aškerčeva 7, 1000 Ljubljana, Slovenia

^bNational Institute of Chemistry, Laboratory for Molecular Modeling, Hajdrihova ulica 19, 1001 Ljubljana, Slovenia

^cUniversity of Helsinki, Faculty of Pharmacy, Division of Pharmaceutical Biosciences, P.O. Box 56, FI-00014 Helsinki, Finland

*Corresponding author:

Žiga Jakopin

Phone: +386 1 4769 646

Fax: + 386 1 4258 031

E-mail address: ziga.jakopin@ffa.uni-lj.si

Abstract :

DNA gyrase and topoisomerase IV are type IIa topoisomerases that are essential bacterial enzymes required to oversee the topological state of DNA during transcription and replication processes. Their ATPase domains, GyrB and ParE, respectively, are recognized as viable targets for small molecule inhibitors, however, no synthetic or natural product GyrB/ParE inhibitors have so far reached the clinic for use as novel antibacterial agents, except for novobiocin which was withdrawn from the market. In the present study, a series of substituted oxadiazoles have been designed and synthesized as potential DNA gyrase inhibitors. Structure-based optimization resulted in the identification of compound **35**, displaying an IC₅₀ of 1.2 μ M for *Escherichia coli* DNA gyrase, while also exhibiting a balanced low micromolar inhibition of *E. coli* topoisomerase IV and of the respective *Staphylococcus aureus* homologues. The most promising inhibitors identified from each series were ultimately evaluated against selected Gram-positive and Gram-negative bacterial strains, of which compound **35** inhibited *Enterococcus faecalis* with a MIC₉₀ of 75 μ M. Our study thus provides further insight into the structural requirements of substituted oxadiazoles for dual inhibition of DNA gyrase and topoisomerase IV.

Keywords:

1,2,4-Oxadiazoles, DNA gyrase inhibition, topoisomerase IV inhibition, Antibacterial screening, Computer-aided drug design

1. INTRODUCTION

The incidence of infections resistant to all currently used antibacterial drugs has increased dramatically in the past decade [1]. The emerging resistance extends to both Gram-positive and Gram-negative organisms and constitutes a serious threat to successful antibacterial therapy [2]. One approach to tackling this issue successfully is to develop novel agents that inhibit known and novel bacterial targets via unique binding sites or via novel modes of action [3].

DNA gyrase and topoisomerase IV are bacterial type IIa topoisomerases and pivotal enzymes required in overseeing the topological state of DNA during transcription and replication processes [4]. While DNA gyrase is essential for the initiation of DNA replication, elongation of nascent DNA and the negative supercoiling of DNA during replication, topoisomerase IV is involved primarily in DNA decatenation at the end of replication [5]. The inhibition of one or both of these enzymes results in the disruption of DNA synthesis, in turn leading to cell death. DNA gyrase and topoisomerase IV are heterotetramers, formed by association of subunits GyrA and GyrB or ParC and ParE, respectively [6-8]. DNA gyrase and topoisomerase IV are clinically validated targets, their druggability being well established in two classes of antibiotics - the fluoroquinolones and aminocoumarins. The fluoroquinolones interact with the GyrA and ParC domain, while aminocoumarins target the GyrB and ParE domains [9]. Of note, DNA gyrase and topoisomerase IV enzymes act in an ATP-dependent manner, relying on their ATPase domains, GyrB and ParE, respectively, for providing the energy required for the extensive conformational changes [6]. Their ATP binding pockets exhibit high homology among bacteria, but at the same time low homology with eukaryotes [4]. They have been recognized early on as potential targets for small molecule inhibitors [7,10,11], however, to date, no synthetic or natural product GyrB/ParE inhibitors since

novobiocin which was withdrawn from the market have reached the clinic due to different issues such as resistance, toxicity and permeability [12]. The GyrB/ParE ATP-binding subunits, therefore, are still insufficiently exploited targets for the development of novel antibacterial agents [13].

Novobiocin and clorobiocin belong to a class of structurally closely related naturally occurring antibiotics, the aminocoumarins (see Fig. 1). Clorobiocin features a pyrrole moiety replacing the carbamate group of novobiocin and a chlorine atom instead of a methyl group. The most essential interaction between these aminocoumarins and the ATP-binding site is achieved in *E. coli* via Asp73 residue and the associated water molecule [7]. Cyclothialidines (see Fig. 1) constitute the second class of naturally occurring DNA gyrase ATPase inhibitors [14-16]. These provide proof of tolerance of the ATP binding site of DNA gyrase to significant chemical diversity [7]. The X-ray crystal structures of coumarins and cyclothialidines bound to the ATP-binding pocket of DNA gyrase further have reinforced that conclusion, revealing that the carbamate of novobiocin, the 2-carboxypyrrole of clorobiocin, and the phenol group of cyclothialidine, are all able to interact with the Asp73 residue and its hydrogen-bonded conserved water molecule [6].

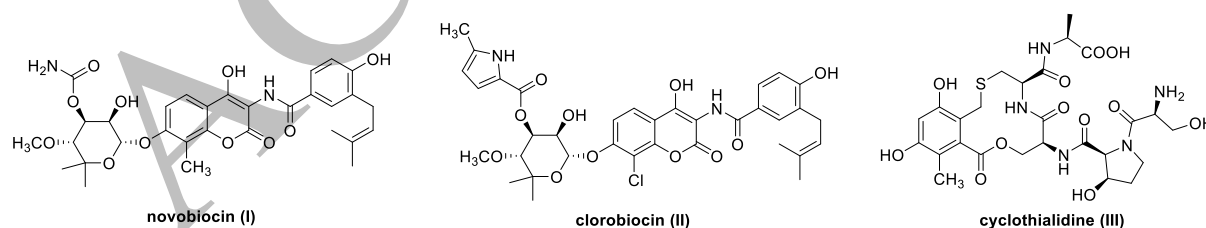


Figure 1. Naturally occurring DNA gyrase inhibitors

The crystal structure of DNA gyrase B was first solved by Wigley in 1991, laying the groundwork for further research in this field [17]. The X-ray structure information on the binding modes of cyclothialidine and novobiocin to the ATP binding site of GyrB [18,19] as

well as the ligand-based inhibitor design [15,16] had established a broad knowledge of the structure-activity relationships (SAR), providing a strong basis for the rational design of novel inhibitors and at the same time enabling further optimization of lead structures.

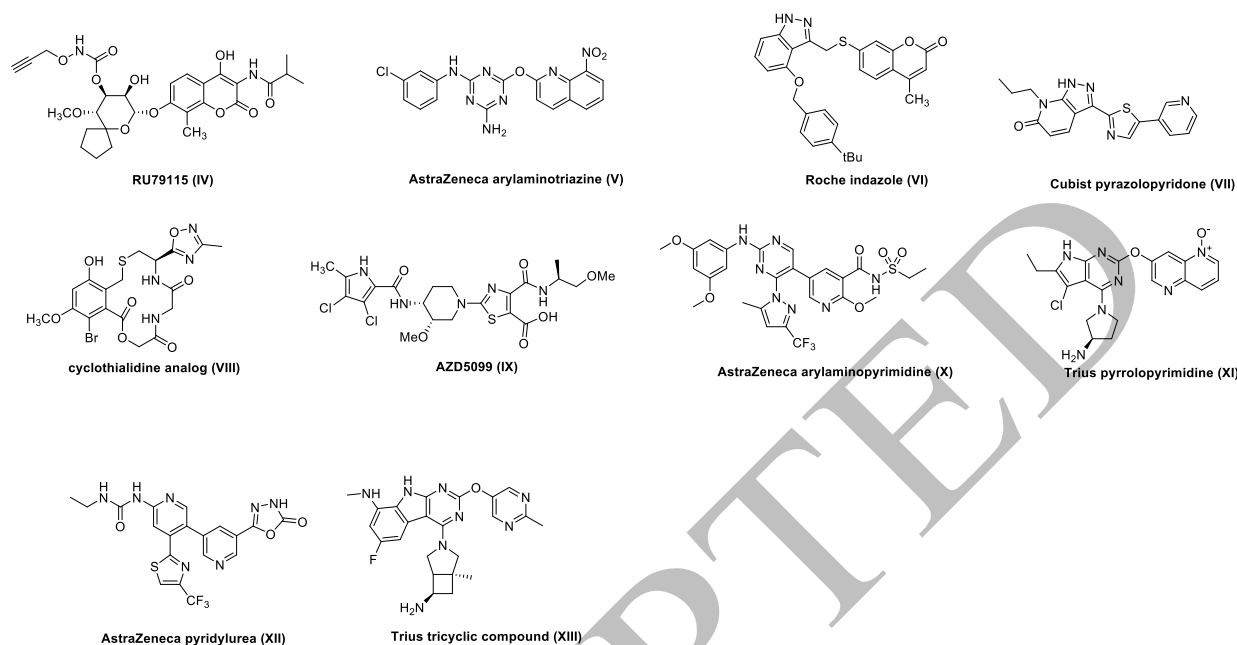


Figure 2. Representative examples of synthetic DNA gyrase and/or topoisomerase IV inhibitors.

The binding modes of the reported inhibitors revealed an overlapping site of interaction, namely a set of hydrogen bonds provided by Asp73 and an associated conserved water molecule. This interaction is essential, and almost indispensable. Nevertheless, other unique structural and electronic characteristics of the binding-site pocket have also been taken into account in the design process. The common structural features of synthesized inhibitors also include functionalities making use of interactions with (i) Arg136; (ii) an additional hydrophobic pocket composed of Val71, Val43, Val167, and Ala147; (iii) a hydrophobic floor consisting of Pro79, Ile78 and Ile94 and (iv) and a π -stacking ceiling formed by Arg76 in a Glu50-Arg76 salt bridge. The ligand-based and fragment-based approaches as well as the targeted screening programs have identified numerous GyrB inhibitors with diverse scaffolds, such as novobiocin and cyclothalididine analogs [15,16,20], arylaminotriazines [21],

arylamino pyrimidines [2], indazoles [22], pyrazolopyridones [23], pyrrolopyrimidines [11,13], pyridylureas [24], pyrrolamides [25] and tricyclic pyrimidinoindoles [26], thus providing several additional starting points for medicinal chemists (structures are shown in Fig. 2).

Currently, there is a pressing need for new antibacterial compounds [27]. Compound **XIV** (Fig. 3), a low nanomolar GyrB inhibitor based on a thiazole-piperidine central core has recently been disclosed as part of a series of promising pyrrolamide GyrB inhibitors [9]. Its development, however, was discontinued mostly due to unfavorable pharmacokinetics. Therefore, we explored possible replacements of the thiazole-piperidine core of **XIV** to find another scaffold that could provide different SAR and optimization opportunities. Oxadiazoles are considered important constituents of biologically active compounds, exhibiting a wide range of effects, which makes them attractive building blocks for a variety of purposes [28-30]. The main objective of the present study was to identify small molecule inhibitors of DNA gyrase based on a novel phenyl-substituted oxadiazole central scaffold by utilising their structural similarity to the known pyrrolamide **XIV**.

2. RESULTS AND DISCUSSION

2.1 Design

Our design was based on the structures of the recently disclosed series of pyrrolamide GyrB inhibitors carrying a thiazole-piperidine central core and represented by compound **XIV** [9]. Making use of both ligand-based as well as structure-based approaches, we chose this inhibitor as lead and designed a small library of its analogs based on a substituted 5-phenyl-1,2,4-oxadiazole central scaffold (Fig. 3). The thiazole-carboxylic acid moiety was bioisosterically replaced by an oxadiazole-carboxylic acid. The aromatic nature of this

heterocycle is key for optimizing π -stacking with Arg76 and hydrogen bond interactions with Arg136, while the pendant carboxylic acid function provides an additional interaction with Arg136. The Glu50-Arg76 salt bridge has also been taken into account, as it is prone to a π -cation interaction with the oxadiazole moiety of the inhibitors.

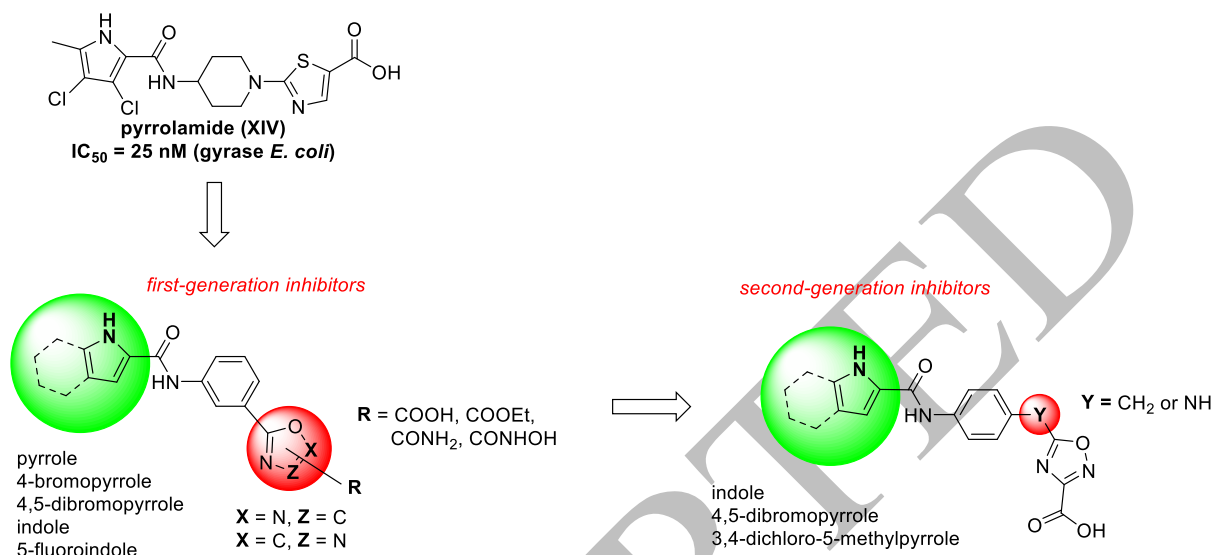


Figure 3. Design of oxadiazole-based DNA gyrase inhibitors.

The pyrrole NH group of **XIV** has been shown to interact with the Asp73-water H-bond motif in the GyrB ATP-binding pocket, indicating a certain degree of similarity of this series to clorobiocin and kibdelomycin [31]. Of note, some of the reported ATP-competitive DNA gyrase inhibitors (e.g. clorobiocin) feature substituted pyrrole moieties in their structures. It has been demonstrated that, by attaching small lipophilic groups to the pyrrole ring, stronger interactions with the left-hand side lipophilic pocket of GyrB can be achieved. Similarly, several DNA gyrase inhibitors possessing pyrrole, dibromopyrrole and bromopyrrole moieties in their structures have been identified [32-36]. Thus, the 5-methyl-3,4-dichloropyrrole moiety of the parent compound was replaced by various heterocyclic moieties, such as indole, pyrrole, 4-bromopyrrole, 4,5-dibromopyrrole and 5-fluoroindole moieties to probe the chemical space of the left-hand side lipophilic pocket. The selection of compounds for the synthesis was guided and corroborated by molecular docking of candidate molecules into the

DNA gyrase ATP-binding site (PDB code: 4DUH). Analysis of the results of molecular docking of compound **19** in the ATP-binding site of *E. coli* DNA gyrase revealed possible hydrophobic interactions of the indole moiety in the hydrophobic pocket formed by Val43, Val71, Val120 and Val167.

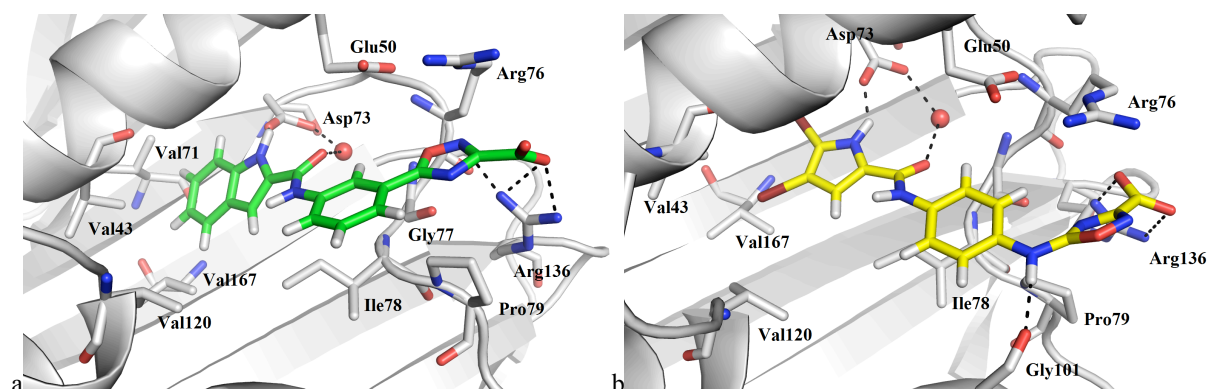


Figure 4. The binding mode of inhibitors a) **19** (in green sticks) and b) **34** (in yellow sticks) in the ATP-binding site of *E. coli* DNA gyrase B (PDB code: 4DUH) as predicted by docking with LeadIT [37]. The ligand and neighboring protein side chains are colored according to the chemical atom type (C₁₉ in green, C₃₄ in yellow, C_{GyrB} in gray, N in blue, O in red, and Br in brown). Hydrogen bonds are indicated by black dotted lines. Figure was prepared by PyMOL [38].

Moreover, **19** was also predicted to form two hydrogen bonds – one with Asp73 side chain and the other with the conserved water molecule bridged to Asp73 carboxylate. In addition, the oxadiazole nucleus is predicted to form cation- π interaction with Arg76 side chain, further reinforcing the binding, while it also forms a hydrogen bond with Arg136 side chain (Fig. 4a). The terminal carboxylate bound to the oxadiazole ring was predicted to form two additional hydrogen bonds with Arg136, thus additionally constraining the inhibitor in the binding site (Fig. 4a).

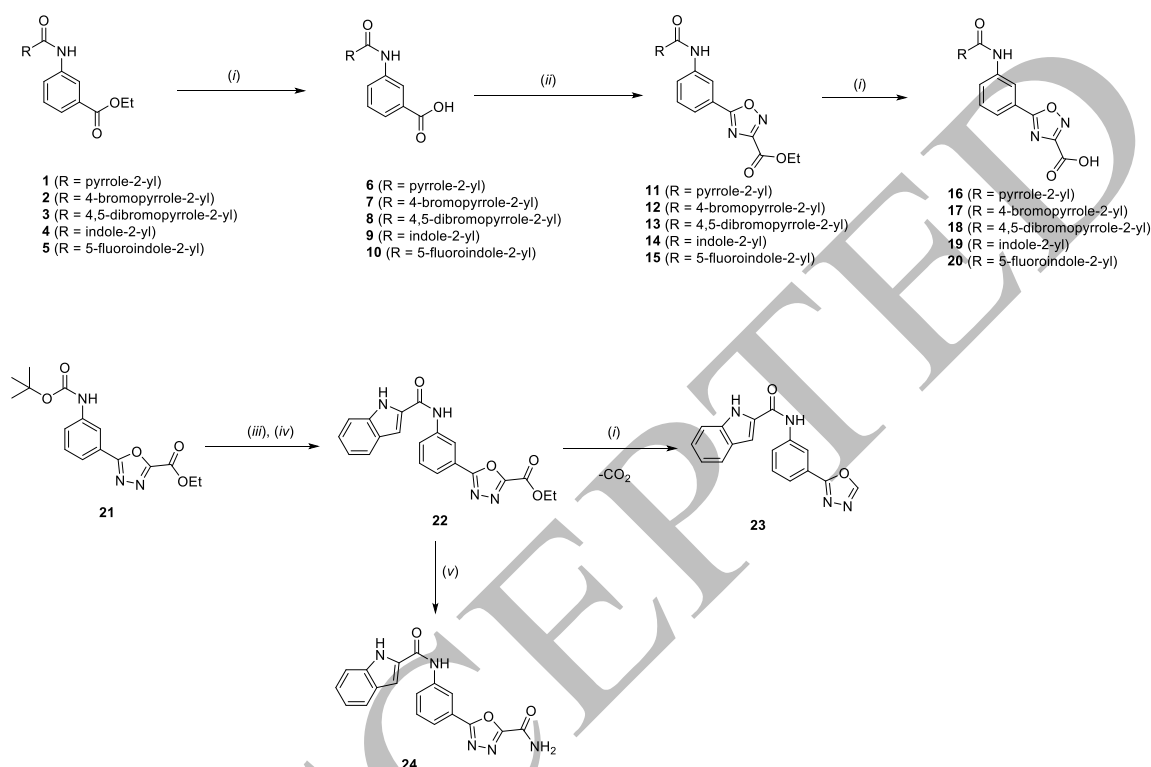
Synthesis of the second series of compounds was also guided by molecular docking of candidate molecules into the DNA gyrase ATP-binding site. These compounds feature a methylene/imine linker connecting the phenyl and 1,2,4-oxadiazole moieties, inserted in the

central scaffold. By inserting a flexible linker, we attempted to direct the carboxylic acid functionality toward the Arg136 in the binding site, as predicted by molecular docking of compound **34** (Fig. 4b). In this case, the imine hydrogen was predicted to form an additional hydrogen bond with Gly101, as seen in the case of GyrB inhibitors discovered by Brvar et al [39]. The indole, 4,5-dibromopyrrole and 5-methyl-3,4-dichloropyrrole moieties, which proved to be the most appropriate to fit the left-hand side hydrophobic pocket of DNA gyrase, have been retained in the structures of this novel series of inhibitors (Fig. 3).

2.2 Chemistry

The starting esters **1-5** were obtained by coupling the corresponding carboxylic acids with ethyl *m*-aminobenzoate using the standard TBTU methodology. The subsequent alkaline hydrolysis of esters **1-5** yielded the acylated derivatives of *m*-aminobenzoic acid **6-10**. The latter were coupled with ethyl 2-oximinooxamate (Scheme 1) using TBTU-coupling conditions (adapted from [40]). The afforded O-acyl amidoximes were immediately subjected to cyclization conditions using KF in 1,4-dioxane at 110 °C, thereby giving the corresponding ethyl 1,2,4-oxadiazole-3-carboxylates **11-15**. Final deprotection of ethyl esters was achieved by alkaline hydrolysis using 1M NaOH/THF mixture [41], affording the final compounds, the 1,2,4-oxadiazole-3-carboxylic acids **16** (pyrrole derivative), **17** (4-bromopyrrole derivative), **18** (4,5-dibromopyrrole derivative), **19** (indole derivative) and **20** (5-fluoroindole derivative). A different path was chosen for the synthesis of the 1,3,4-oxadiazole-incorporating congeners (outlined in Scheme 1). The key intermediate amine **21**, synthesized as described [42], was *N*-deprotected under acidolytic conditions and then coupled with indole-2-carboxylic acid using TBTU-coupling conditions to afford the corresponding amide **22**. Deprotection of ethyl 1,3,4-oxadiazole-2-carboxylate **22** was achieved by alkaline hydrolysis using 1M NaOH/THF mixture, but the compound underwent a decarboxylation and instead of affording the desired

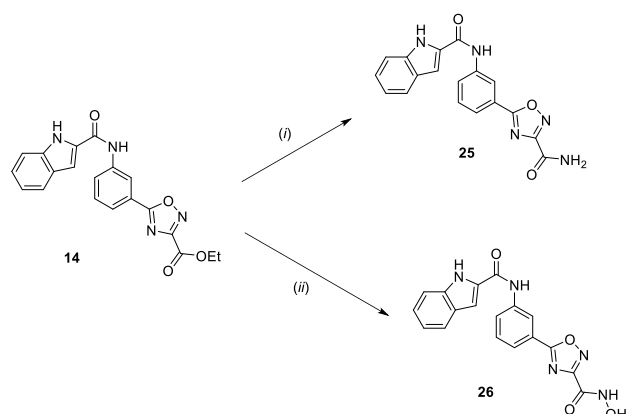
1,3,4-oxadiazole-2-carboxylic acid, the decarboxylated derivative **23** was formed. Compound **22** was further derivatized into a more stable amide derivative **24**. Aminolysis of ethyl ester **22** was achieved by bubbling ammonia gas through its ethanolic solution at 0 °C, thereby achieving complete conversion to the amide derivative **24**.



Scheme 1. Synthesis of oxadiazole-based DNA gyrase inhibitors. Reagents and conditions: (i) 1M NaOH/THF; (ii) a) ethyl 2-oximinooxamate, TBTU, DIPEA, DMAP, CH₂Cl₂ b) KF, 1,4-dioxane, 110 °C; (iii) TFA/CH₂Cl₂ (1:5); (iv) indole-2-carboxylic acid, TBTU, DIPEA, DMAP, CH₂Cl₂, reflux; (v) NH₃ (g)/EtOH, 0 °C.

Compound **14** was further derivatized to its corresponding amide derivative **25** as well as its hydroxamic acid derivative **26** (Scheme 2). Aminolysis of ethyl ester **14** was achieved by bubbling ammonia gas through an ethanolic solution of the compound at 0 °C. Hydroxamic acid **26** was synthesized by a different route [40]. Compound **14** was dissolved in methanol; a methanolic solution of hydroxylamine was then added, followed by the addition of a catalytic

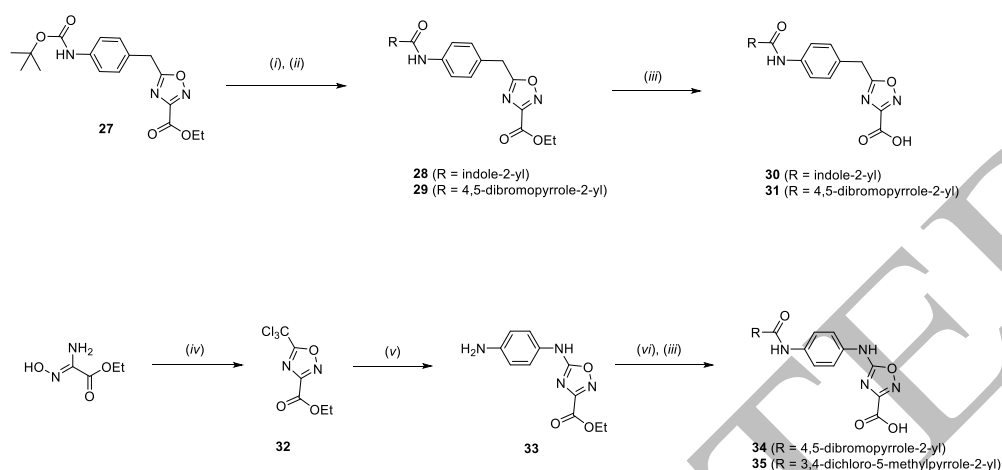
amount of KCN. The reaction mixture was stirred at room temperature until the starting compound was completely converted to the hydroxamic acid derivative **26**.



Scheme 2. Synthesis of carboxamide and hydroxamic acid derivatives of **14**. Reagents and conditions: (i) NH_3 (g)/EtOH, 0 °C; (ii) $\text{NH}_2\text{OH}\times\text{HCl}$, KOH, KCN, MeOH.

Synthesis of the second-generation oxadiazole-based DNA gyrase inhibitors is presented in Scheme 3. The key intermediate ethyl 1,2,4-oxadiazole-3-carboxylate **27** was synthesized as described previously [42]. Subsequently, *N*-Boc protecting group was removed under acidolytic conditions, giving the free amine intermediate which was then coupled with different acids (indole-2-carboxylic acid and 4,5-dibromopyrrole-2-carboxylic acid) using TBTU-coupling conditions to afford the corresponding amides **28** and **29**. Deprotection of esters was achieved by alkaline hydrolysis using 1M NaOH/THF mixture, affording the end compounds 1,2,4-oxadiazole-3-carboxylic acids **30** (indole derivative) and **31** (4,5-dibromopyrrole derivative). Compounds **34** and **35** were synthesized by a different route (Scheme 3). First, ethyl 2-oximinooxamate was reacted with trichloroacetic acid anhydride (TCAA) at 140 °C for 3 h, yielding the 5-trichloromethyl-1,2,4-oxadiazole intermediate [43]. In the following step, the 5-trichloromethyl derivative **32** underwent a nucleophilic displacement with *p*-phenylenediamine in the presence of DMAP in refluxing chloroform to afford compound **33** (adapted by [44]). The latter was then coupled with 4,5-dibromopyrrole-2-carboxylic acid or 3,4-dichloro-5-methylpyrrole-2-carboxylic acid using TBTU-coupling

conditions to afford the corresponding amides which were immediately used in the next step, namely alkaline hydrolysis using 1M NaOH/THF mixture, affording the end compounds **34** and **35**.



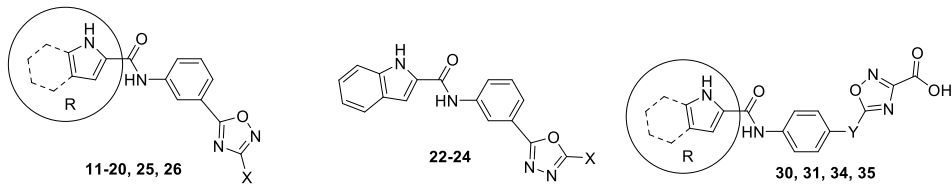
Scheme 3. Synthesis of second-generation oxadiazole based DNA gyrase inhibitors. Reagents and conditions: (i) TFA/CH₂Cl₂ (1:5); (ii) indole-2-carboxylic acid or 4,5-diBr-pyrrole-2-carboxylic acid, TBTU, DIPEA, DMAP, CH₂Cl₂, reflux; (iii) 1M NaOH/THF; (iv) trichloroacetic acid anhydride, 140 °C; (v) *p*-phenylenediamine, DMAP, chloroform, reflux; (vi) 4,5-diBr-pyrrole-2-carboxylic acid or 3,4-diCl-5-methylpyrrole-2-carboxylic acid, TBTU, DIPEA, DMAP, CH₂Cl₂.

2.3 Biological data

2.3.1 *In vitro* enzyme inhibition

Initial screening of the first series of compounds in the *E. coli* DNA gyrase supercoiling assay comprising GyrA and GyrB subunits of DNA gyrase (Table 1) highlighted the importance of the indole moiety for DNA gyrase inhibition in concert with the free carboxylic acid functionality located on the 1,2,4-oxadiazole nucleus, as seen in the case of the best inhibitor of this series **19** [IC₅₀ = 4.0 μM].

Table 1. Inhibitory activities of oxadiazole-based inhibitors

							
compound	R	X	Y	DNA gyrase		topoisomerase IV	
				RA [%] ^{a, b} or IC ₅₀ [μM]		RA [%] ^{a, b} or IC ₅₀ [μM]	
				<i>E. coli</i>	<i>S. aureus</i>	<i>E. coli</i>	<i>S. aureus</i>
novobiocin ^c	-	-	-	0.17 μM	0.040 μM	11 μM	27 μM
11	pyrrole-2-yl	COOEt	-	86%	nd	nd	nd
12	4-Br-pyrrole-2-yl	COOEt	-	71 %	nd	nd	nd
13	4,5-diBr-pyrrole-2-yl	COOEt	-	98 %	nd	nd	nd
14	indole-2-yl	COOEt	-	97%	nd	nd	nd
15	5-F-indole-2-yl	COOEt	-	148%	nd	nd	nd
16	pyrrole-2-yl	COOH	-	92%	nd	nd	nd
17	4-Br-pyrrole-2-yl	COOH	-	61%	nd	nd	nd
18	4,5-diBr-pyrrole-2-yl	COOH	-	61 μM	nd	nd	nd
19	indole-2-yl	COOH	-	4.0 μM	88%	100%	88%
20	5-F-indole-2-yl	COOH	-	144 %	nd	nd	nd
22	-	COOEt	-	133 %	nd	nd	nd
23	-	H	-	106%	nd	nd	nd
24	-	CONH ₂	-	81 %	nd	nd	nd
25	indole-2-yl	CONH ₂	-	91 %	nd	nd	nd
26	indole-2-yl	CONHOH	-	92 %	nd	nd	nd
30	indole-2-yl	-	CH ₂	82%	nd	nd	nd
31	4,5-diBr-pyrrole-2-yl	-	CH ₂	66 μM	nd	nd	nd
34	4,5-diBr-pyrrole-2-yl	-	NH	5.8 μM	nd	nd	nd
35	3,4-diCl-5-methylpyrrole-2-yl	-	NH	1.2 μM	12 μM	135 μM	15 μM

^aResidual activity of the enzyme at 100 μM of the tested compound.^b1% DMSO was used as a negative control.^cnovobiocin was used as a positive control.^dn.d. – not determined.

The importance of hydrophobic interactions of the inhibitors was further supported by the inactivity of the pyrrole analogue **16** and weak activity of the 4-bromopyrrole-based compound **17** [$IC_{50} > 100 \mu M$]. Their 4,5-dibromopyrrole congener **18** [$IC_{50} = 61 \mu M$] possessed 15-fold weaker inhibitory activity than compound **19**. Hydrophobic pocket of the ATP-binding site of *E. coli* GyrB was further probed by the 5-fluoroindole-based **20**, however the resulting compound displayed a complete lack of activity, indicating that the 5-fluoroindole moiety is most likely too large to fit into this pocket. The ethyl esters **11** (pyrrole-based), **12** (4-bromopyrrole-based), **13** (4,5-dibromopyrrole-based), **14** (indole-based) and **15** (5-fluoroindole-based) were completely devoid of inhibitory activity. Based on the results of this preliminary screening, compound **19** was selected for further exploration of its chemical space. Interestingly, its carboxamide analog **25** and its hydroxamic acid analog **26** were completely devoid of any inhibitory activity. Synthesis of the regioisomer of 1,2,4-oxadiazole **19**, incorporating the 1,3,4-oxadiazole moiety, was also attempted via alkaline hydrolysis of the corresponding ethyl ester analog **22**. The free 1,3,4-oxadiazole-3-carboxylic acid however proved unstable and underwent an immediate decarboxylation, affording the des-carboxy derivative **23**. The obtained des-carboxy derivative **23** and ester **22** were devoid of any inhibitory activity. The carboxamide regioisomer of **25**, compound **24**, was also prepared and also showed no inhibitory activity.

Screening of the second-generation of compounds (see Table 1) highlighted the importance of the 4,5-dibromopyrrole moiety and the free carboxylic acid functionality for DNA gyrase inhibition. Interestingly, as opposed to the results of the first generation of compounds, the indole-based and methylene linker-containing free acid **30** was completely devoid of inhibitory activity, while its 4,5-dibromopyrrole-incorporating counterpart **31** [$IC_{50} = 66 \mu M$] was moderately inhibitory active. The best inhibitors of the second-generation of compounds

were compounds carrying the imine linker, namely compounds **34** [$IC_{50} = 5.8 \mu M$] and **35** [$IC_{50} = 1.2 \mu M$]. Comparing **34** to its methylene linker analog **31**, it becomes evident that the ability to form an additional hydrogen bond with Gly101 (as shown in Fig. 4b) is reflected in a 10-fold lower IC_{50} value. On the other hand, the new 3,4-dichloro-5-methylpyrrole moiety featured in compound **35** further increased hydrophobic interactions in the adenine pocket, resulting in slightly stronger inhibitory activity than **34**. Moreover, the flexible imine linker orients the carboxylic acid moieties of **34** and **35** to face the Arg136 side chain, forming two hydrogen bonds and resulting in stronger inhibitory activities of these two inhibitors than **19** and **18**. The best compounds of each series, compounds **19** and **35**, were additionally tested for their potential inhibition of *E. coli* topoisomerase IV and of *Staphylococcus aureus* DNA gyrase and topoisomerase IV homologs. Compound **19** was inactive, while the 3,4-dichloro-5-methylpyrrole-based oxadiazole inhibitor **35** showed promising inhibitory activity against all four tested enzymes in the micromolar range (IC_{50} values from 1.2 to 135 μM). The inhibitory potencies of **35** against DNA gyrase [IC_{50} (*E. coli*) = 1.2 μM] and topoisomerase IV [IC_{50} (*E. coli*) = 135 μM] from *E. coli* were approximately 10-fold lower than those of novobiocin. Nevertheless, for the *S. aureus* enzymes, the IC_{50} values were more comparable. In fact, inhibition of topoisomerase IV by **35** [IC_{50} (*S. aureus*) = 15 μM] was even better than that of novobiocin [IC_{50} (*S. aureus*) = 27 μM], while the reverse was the case for DNA gyrase [**35**: IC_{50} (*S. aureus*) = 12 μM ; novobiocin: (IC_{50} (*S. aureus*) = 0.040 μM)].

2.3.2 Antibacterial activity

Oxadiazoles **18**, **19** and **35** were tested against two Gram-positive (*Staphylococcus aureus* ATCC 25923, *Enterococcus faecalis* ATCC 29212) and two Gram-negative (*Escherichia coli* ATCC 25922, *Pseudomonas aeruginosa* ATCC 27853) bacterial strains. In general, the compounds exhibited no significant antibacterial activities against Gram-positive bacteria and

only a weak growth inhibition of *S. aureus* (inhibitions $\leq 38\%$ at $50\ \mu\text{M}$ concentration; data not shown). The only notable activity was observed against *E. faecalis* for compound **35** which showed $>80\%$ inhibition of the growth of *E. faecalis* in the primary screen at $50\ \mu\text{M}$ and the MIC_{90} determined by dose-response experiments was $75\ \mu\text{M}$. None of the compounds showed any antibacterial activity against the tested Gram-negative bacteria. Further optimization of physicochemical properties of compounds and their enzyme inhibitory activities are needed to transform these compounds into inhibitors with improved antibacterial activity.

3. CONCLUSIONS

In conclusion, two series of substituted oxadiazoles have been prepared originating from the structure **XIV**. Iterative cycles of structure-based optimization resulted in compound **35** which displayed an IC_{50} of $1.2\ \mu\text{M}$ of *E. coli* DNA gyrase and proved to be the most potent of the series. The docking experiments suggest that this class of inhibitors bind to the ATP-binding site of the enzyme. It is noteworthy, that compound **35** also exhibited a balanced micromolar inhibition of *E. coli* topoisomerase IV and of the *Staphylococcus aureus* homologs. Furthermore, it also exhibited a modest inhibition against *Enterococcus faecalis* ($\text{MIC}_{90} = 75\ \mu\text{M}$). Overall, the results offer a valuable insight into the structural requirements of substituted oxadiazoles for DNA gyrase inhibition and thus provide a good foundation for further research in this field.

4. EXPERIMENTAL SECTION

4.1 Materials and methods

Chemicals were obtained from Acros, Sigma-Aldrich and TCI, and used without further purification. Analytical TLC was performed on Merck 60 F254 silica gel plates ($0.25\ \text{mm}$),

using visualization with ultraviolet light and ninhydrin. Column chromatography was carried out on silica gel 60 (particle size 240-400 mesh). Melting points were determined on a Reichert hot stage microscope and are uncorrected. ^1H - and ^{13}C -NMR spectra were recorded at 400 MHz and 100 MHz, respectively, on a Bruker AVANCE III spectrometer in $\text{DMSO-}d_6$, MeOD or CDCl_3 solution with TMS as the internal standard. Spectra were assigned using gradient HSQC and HMBC techniques. IR spectra were recorded on a Perkin-Elmer 1600 FT-IR spectrometer. Mass spectra were obtained using a VG-Analytical Autospec Q mass spectrometer. Microanalyses were performed on a 240 C Perkin-Elmer CHN analyzer. HPLC analyses were performed on an Agilent Technologies HP 1100 instrument with G1365B UV-VIS detector (254 nm), using a Luna C18 column (4.6×150 mm) at a flow rate of 1 mL/min. The eluent was a mixture of 0.1% TFA in water (A) and acetonitrile (B), with a gradient of 30% B to 80% B from 0-30 minutes and 80% B to 90% B from 30-33 minutes.

4.2 General procedures

4.2.1 Formation of 1,2,4-oxadiazoles

To a stirred solution of carboxylic acid derivative (1.0 eq) in dried tetrahydrofuran (THF), diisopropylethylamine (3.0 eq) and 2-(1*H*-benzotriazol-1-yl)-1,1,3,3-tetramethyluronium tetrafluoroborate (TBTU) (1.1 eq) were added. After stirring for 45 minutes ethyl 2-oximinooxamate (1.0 eq) and a catalytic amount of 4-dimethylaminopyridine (DMAP) (0.1 eq) were added and the mixture stirred at room temperature for an additional 2 h. The solvent was then removed in vacuo to afford the crude product. This was used without purification in the next step in which it was dissolved in dry 1,4-dioxane (5 mL). Potassium fluoride (3.0 eq) was then added and the mixture was heated at 80 °C for 24 h. On completion, the reaction mixture was concentrated in vacuo and the residue purified by flash silica gel column

chromatography (gradient elution; starting eluent: hexane/ethyl acetate 3:1 v/v) to afford the desired compounds **11-15**.

4.2.2 Acidolytic cleavage of Boc protecting groups and the subsequent TBTU-mediated coupling

To an ice-chilled stirred mixture of trifluoroacetic acid (TFA) and dichloromethane (v/v 1/5, 5 mL) Boc-protected compound (1.0 eq) was added and the mixture allowed to warm to room temperature. After 3 h the reaction was complete and the solvent was evaporated in vacuo. The residue was washed three times with diethyl ether giving a crude ammonium salt which was dissolved in dichloromethane followed by the addition of diisopropylethylamine (1.0 eq). In a parallel reaction, to a stirred solution of indole-2-carboxylic acid or 4,5-dibromo-pyrrole-2-carboxylic acid (1.0 eq) in dry dichloromethane (10 mL), diisopropylethylamine (3.0 eq) and TBTU (1.1 eq) were added. After stirring for 45 minutes the solution of free amine in dichloromethane was added at 0 °C, and the mixture was allowed to warm to room temperature. Stirring was continued for 48 h. On completion, the reaction mixture was diluted with dichloromethane (30 mL) then washed with 1M HCl (2 × 20 mL), water (20 mL), saturated NaHCO₃ solution (2 × 20 mL), water (20 mL) and dried over anhydrous Na₂SO₄. The solvent was concentrated in vacuo and the residue purified by flash silica gel column chromatography (gradient elution; starting eluent: hexane/ethyl acetate 2:1 v/v) to afford the corresponding amides **22**, **28** and **29**.

4.2.3 TBTU-mediated coupling

To a stirred solution of carboxylic acid (1.0 eq) in dry dichloromethane (10 mL), diisopropylethylamine (3.0 eq) and TBTU (1.1 eq) were added. After stirring for 45 minutes ethyl *m*-aminobenzoate was added at 0 °C, and the mixture allowed to warm to room

temperature; stirring then continued for 48 h. On completion, the reaction mixture was diluted with dichloromethane (30 mL) then washed with 1M HCl (2×20 mL), water (20 mL), saturated NaHCO₃ solution (2×20 mL), water (20 mL) and dried over anhydrous Na₂SO₄. The solvent was concentrated in vacuo to afford the desired amides **1-5**.

4.2.4 Alkaline hydrolysis

To a solution of the corresponding ester (1 eq) in THF, 1M NaOH (5 eq) was added and the reaction mixture stirred at room temperature for 5 h. THF was evaporated under vacuum and the resulting aqueous solution neutralized with 1M HCl until the product started to precipitate. The product was filtered off, then dried to afford the desired acids **6-10**.

4.3 Characterization of compounds

4.3.1 Ethyl 3-(1H-pyrrole-2-carboxamido)benzoate (1). Synthesized according to the general procedure for TBTU-mediated coupling. Beige amorphous powder; m.p. 158-160 °C. ¹H-NMR (DMSO-d₆, 400 MHz): δ = 1.34 (t, 3H, J = 7.2 Hz, -CH₂-CH₃), 4.34 (q, 2H, J = 7.2 Hz, -CH₂-CH₃), 6.18-6.20 (m, 1H, Ar-H), 6.99-7.00 (m, 1H, Ar-H), 7.11-7.13 (m, 1H, Ar-H), 7.48 (t, 1H, J = 8.0 Hz, Ar-H), 7.64-7.66 (m, 1H, Ar-H), 8.07-8.10 (m, 1H, Ar-H), 8.38 (t, 1H, J = 2.0 Hz, Ar-H), 9.98 (s, 1H, -CONH), 11.71 (s, 1H, pyrrole-NH) ppm. MS (ESI): m/z (%) = 259.1 (M+H)⁺. IR (KBr): ν = 3330, 2982, 1760, 1714, 1628, 1594, 1549, 1529, 1439, 1403, 1366, 1333, 1317, 1283, 1264, 1233, 1159, 1130, 1096, 1047, 1023, 1000, 946, 904, 741, 682, 671, 603 cm⁻¹. HRMS Calcd for C₁₄H₁₅N₂O₃ m/z : 259.1083 (M+H)⁺, found 259.1077.

4.3.2 Ethyl 3-(4-bromo-1H-pyrrole-2-carboxamido)benzoate (2). Synthesized according to the general procedure for TBTU-mediated coupling. Beige amorphous powder; m.p. 208-211 °C. ¹H-NMR (DMSO-d₆, 400 MHz): δ = 1.34 (t, 3H, J = 7.2 Hz, -CH₂-CH₃), 4.34 (q, 2H, J =

7.2 Hz, -CH₂-CH₃), 7.13-7.15 (m, 1H, Ar-H), 7.21-7.22 (m, 1H, Ar-H), 7.50 (t, 1H, *J* = 8.0 Hz, Ar-H), 7.67 (dd, 1H, *J* = 8.0 Hz, *J* = 1,2 Hz, Ar-H), 8.05-8.08 (m, 1H, Ar-H), 8.37 (t, 1H, *J* = 2.0 Hz, Ar-H), 10.04 (s, 1H, -CONH), 12.11 (s, 1H, pyrrole-NH) ppm. ¹³C-NMR (DMSO-d₆, 100 MHz): δ = 14.16, 60.78, 95.28, 112.97, 120.25, 122.67, 123.79, 124.16, 126.33, 129.10, 130.31, 139.39, 158.18, 165.59 ppm. MS (ESI): *m/z* (%) = 337.0 (M+H)⁺. IR (KBr): ν = 3387, 3352, 3224, 3123, 2976, 1695, 1652, 1597, 1556, 1534, 1431, 1384, 1365, 1332, 1294, 1263, 1235, 1184, 1141, 1090, 920, 755 cm⁻¹. HRMS Calcd for C₁₄H₁₄BrN₂O₃ *m/z*: 337.0188 (M+H)⁺, found 337.0197.

4.3.3 Ethyl 3-(4,5-dibromo-1H-pyrrole-2-carboxamido)benzoate (3). Synthesized according to the general procedure for TBTU-mediated coupling. Beige amorphous powder; m.p. 235-237 °C. ¹H-NMR (DMSO-d₆, 400 MHz): δ = 1.34 (t, 3H, *J* = 7.2 Hz, -CH₂-CH₃), 4.34 (q, 2H, *J* = 7.2 Hz, -CH₂-CH₃), 7.28 (d, 1H, *J* = 2.4 Hz, Ar-H), 7.50 (t, 1H, *J* = 8.0 Hz, Ar-H), 7.66-7.69 (m, 1H, Ar-H), 8.04-8.07 (m, 1H, Ar-H), 8.35 (t, 1H, *J* = 2.0 Hz, Ar-H), 10.08 (s, 1H, -CONH), 12.97 (s, 1H, pyrrole-NH) ppm. ¹³C-NMR (DMSO-d₆, 100 MHz): δ = 14.16, 60.80, 98.24, 106.23, 114.08, 120.27, 123.93, 124.17, 127.62, 129.16, 130.34, 139.22, 157.43, 165.56 ppm. MS (ESI): *m/z* (%) = 414.9 (M+H)⁺. IR (KBr): ν = 3341, 3175, 3128, 1686, 1651, 1588, 1552, 1523, 1439, 1394, 1287, 1274, 1231, 1183, 752 cm⁻¹. HRMS Calcd for C₁₄H₁₃Br₂N₂O₃ *m/z*: 414.9293 (M+H)⁺, found 414.9302.

4.3.4 Ethyl 3-(1H-indole-2-carboxamido)benzoate (4). Synthesized according to the general procedure for TBTU-mediated coupling. Beige amorphous powder; m.p. 214-217 °C. ¹H-NMR (DMSO-d₆, 400 MHz): δ = 1.36 (t, 3H, *J* = 7.2 Hz, -CH₂-CH₃), 4.35 (q, 2H, *J* = 7.2 Hz, -CH₂-CH₃), 7.09 (t, 1H, *J* = 8.0 Hz, Ar-H), 7.24 (t, 1H, *J* = 8.0 Hz, Ar-H), 7.47-7.49 (m, 2H, Ar-H), 7.54 (t, 1H, *J* = 8.0 Hz, Ar-H), 7.69-7.72 (m, 2H, Ar-H), 8.14-8.17 (m, 1H, Ar-H),

8.46 (t, 1H, $J = 2.0$ Hz, Ar-H), 10.45 (s, 1H, -CONH), 11.79 (s, 1H, indole-NH) ppm. MS (ESI): m/z (%) = 309.1 (M+H)⁺. IR (KBr): $\nu = 3350, 3303, 1686, 1655, 1588, 1536, 1439, 1420, 1395, 1369, 1317, 1290, 1236, 1196, 1168, 1144, 1106, 743, 681$ cm⁻¹. HRMS Calcd for C₁₈H₁₇N₂O₃ m/z : 309.1239 (M+H)⁺, found 309.1233.

4.3.5 Ethyl 3-(5-fluoro-1H-indole-2-carboxamido)benzoate (5). Synthesized according to the general procedure for TBTU-mediated coupling. Beige amorphous powder; m.p. 183-186 °C. ¹H-NMR (DMSO-d₆, 400 MHz): $\delta = 1.34$ (t, 3H, $J = 7.2$ Hz, -CH₂-CH₃), 4.34 (q, 2H, $J = 7.2$ Hz, -CH₂-CH₃), 7.10 (dt, 1H, $J = 9.2$ Hz, $J = 2.4$ Hz, Ar-H), 7.45-7.55 (m, 4H, Ar-H), 7.70 (td, 1H, $J = 8.0$ Hz, $J = 1.2$ Hz, Ar-H), 8.14-8.16 (m, 1H, Ar-H), 8.45 (t, 1H, $J = 2.0$ Hz, Ar-H), 10.51 (s, 1H, -CONH), 11.92 (s, 1H, indole-NH) ppm. MS (ESI): m/z (%) = 325.1 (M-H)⁻. IR (KBr): $\nu = 3347, 3297, 1685, 1655, 1590, 1537, 1439, 1423, 1369, 1283, 1236, 1206, 1146, 1105, 856, 798, 751, 733, 682$ cm⁻¹. HRMS Calcd for C₁₈H₁₅FN₂O₃ m/z : 325.0988 (M-H)⁻, found 325.0990.

4.3.6 3-(1H-pyrrole-2-carboxamido)benzoic acid (6). Synthesized according to the general procedure for alkaline hydrolysis described. Beige amorphous powder; m.p. 234-236 °C. ¹H-NMR (DMSO-d₆, 400 MHz): $\delta = 6.18$ (s, 1H, Ar-H), 6.98 (s, 1H, Ar-H), 7.11 (s, 1H, Ar-H), 7.45 (t, 1H, $J = 8.0$ Hz, Ar-H), 7.63 (d, 1H, $J = 7.6$ Hz, Ar-H), 8.06 (d, 1H, $J = 8.0$ Hz, Ar-H), 8.34 (s, 1H, Ar-H), 9.93 (s, 1H, -CONH), 11.67 (s, 1H, pyrrole-NH), 12.92 (s, 1H, COOH) ppm. MS (ESI): m/z (%) = 229.1 (M-H)⁻. IR (KBr): $\nu = 3336, 2819, 2563, 1689, 1626, 1592, 1551, 1529, 1448, 1395, 1296, 1272, 1167, 1157, 1132, 750$ cm⁻¹. HRMS Calcd for C₁₂H₉N₂O₃ m/z : 229.0613 (M-H)⁻, found 229.0618.

4.3.7 3-(4-Bromo-1H-pyrrole-2-carboxamido)benzoic acid (7). Synthesized according to the general procedure for alkaline hydrolysis. Beige amorphous powder; m.p. 264-266 °C. ¹H-NMR (DMSO-d₆, 400 MHz): δ = 7.12 (s, 1H, Ar-H), 7.20 (s, 1H, Ar-H), 7.46 (t, 1H, *J* = 8.0 Hz, Ar-H), 7.65 (d, 1H, *J* = 7.6 Hz, Ar-H), 8.03 (d, 1H, *J* = 8.0 Hz, Ar-H), 8.33 (s, 1H, Ar-H), 10.00 (s, 1H, -CONH), 12.07 (s, 1H, pyrrole-NH), 12.97 (s, 1H, COOH) ppm. MS (ESI): *m/z* (%) = 307.0 (M-H)⁻. IR (KBr): ν = 3523, 3396, 3284, 2981, 1735, 1695, 1652, 1574, 1540, 1478, 1445, 1419, 1379, 1314, 1274, 1240, 1213, 741, 670 cm⁻¹. HRMS Calcd for C₁₂H₈BrN₂O₃ *m/z*: 306.9718 (M-H)⁻, found 306.9719.

4.3.8 3-(4,5-Dibromo-1H-pyrrole-2-carboxamido)benzoic acid (8). Synthesized according to the general procedure for alkaline hydrolysis. Beige amorphous powder; m.p. 265-268 °C. ¹H-NMR (DMSO-d₆, 400 MHz): δ = 7.26 (s, 1H, Ar-H), 7.44 (t, 1H, *J* = 8.0 Hz, Ar-H), 7.65 (d, 1H, *J* = 7.6 Hz, Ar-H), 8.02 (d, 1H, *J* = 8.4 Hz, Ar-H), 8.30 (s, 1H, Ar-H), 10.02 (s, 1H, -CONH), 12.93 (br s, 2H, COOH, pyrrole-NH) ppm. MS (ESI): *m/z* (%) = 384.9 (M-H)⁻. IR (KBr): ν = 3197, 2864, 1696, 1669, 1550, 1522, 1487, 1436, 1387, 1229, 1178 cm⁻¹. HRMS Calcd for C₁₂H₇Br₂N₂O₃ *m/z*: 384.8823 (M-H)⁻, found 384.8819.

4.3.9 3-(1H-indole-2-carboxamido)benzoic acid (9). Synthesized according to the general procedure for alkaline hydrolysis. Beige amorphous powder; m.p. 268-270 °C. ¹H-NMR (DMSO-d₆, 400 MHz): δ = 7.08 (t, 1H, *J* = 7.6 Hz, Ar-H), 7.24 (t, 1H, *J* = 7.6 Hz, Ar-H), 7.48-7.52 (m, 3H, Ar-H), 7.69 (d, 1H, *J* = 8.0 Hz, Ar-H), 8.13 (d, 1H, *J* = 8.4 Hz, Ar-H), 8.43 (s, 1H, Ar-H), 10.42 (s, 1H, -CONH), 11.78 (s, 1H, indole-NH), 12.99 (s, 1H, COOH) ppm. MS (ESI): *m/z* (%) = 279.1 (M-H)⁻. IR (KBr): ν = 3349, 3009, 2846, 1693, 1638, 1590, 1537, 1486, 1437, 1411, 1340, 1305, 1271, 1231, 1191, 807, 741, 676, 666 cm⁻¹. HRMS Calcd for C₁₆H₁₁N₂O₃ *m/z*: 279.0770 (M-H)⁻, found 279.0775.

4.3.10 3-(5-Fluoro-1H-indole-2-carboxamido)benzoic acid (10). Synthesized according to the general procedure for alkaline hydrolysis. Beige amorphous powder; m.p. 237-240 °C. ¹H-NMR (DMSO-d₆, 400 MHz): δ = 7.09 (dt, 1H, *J* = 9.2 Hz, *J* = 2.4 Hz, Ar-H), 7.45-7.50 (m, 4H, Ar-H), 7.69 (td, 1H, *J* = 7.6 Hz, *J* = 1.2 Hz, Ar-H), 8.12-8.15 (m, 1H, Ar-H), 8.46 (t, 1H, *J* = 1.6 Hz, Ar-H), 10.67 (s, 1H, -CONH), 12.06 (s, 1H, indole-NH) ppm. MS (ESI): *m/z* (%) = 297.1 (M-H)⁻. IR (KBr): ν = 3352, 1694, 1643, 1592, 1542, 1446, 1419, 1330, 1311, 1273, 1252, 1230, 1205, 752, 729, 667 cm⁻¹. HRMS Calcd for C₁₆H₁₀FN₂O₃ *m/z*: 297.0675 (M-H)⁻, found 297.0679.

4.3.11 Ethyl 5-(3-(1H-pyrrole-2-carboxamido)phenyl)-1,2,4-oxadiazole-3-carboxylate (11). Synthesized according to the general procedure for acidolytic cleavage of Boc protecting groups and the subsequent TBTU-mediated coupling. Beige amorphous powder; m.p. 236-238 °C. ¹H-NMR (DMSO-d₆, 400 MHz): δ = 1.36 (t, 3H, *J* = 7.2 Hz, -CH₂-CH₃), 4.45 (q, 2H, *J* = 7.2 Hz, -CH₂-CH₃), 6.19-6.20 (m, 1H, Ar-H), 7.01-7.02 (m, 1H, Ar-H), 7.13-7.14 (m, 1H, Ar-H), 7.62 (t, 1H, *J* = 8.0 Hz, Ar-H), 7.83 (dd, 1H, *J* = 8.4 Hz, *J* = 1.6 Hz, Ar-H), 8.17 (dd, 1H, *J* = 8.0 Hz, *J* = 2.0 Hz, Ar-H), 8.64 (s, 1H, Ar-H), 10.08 (s, 1H, -CONH), 11.74 (s, 1H, pyrrole-NH) ppm. ¹³C-NMR (DMSO-d₆, 100 MHz): δ = 13.88, 62.58, 84.80, 109.10, 111.82, 118.61, 122.12, 123.04, 123.15, 124.32, 125.56, 130.15, 140.54, 157.18, 159.34, 162.12 ppm. MS (ESI): *m/z* (%) = 325.1 (M-H)⁻. IR (KBr): ν = 3335, 1751, 1628, 1567, 1546, 1525, 1487, 1475, 1463, 1444, 1430, 1405, 1276, 1197, 1169, 1130, 1094, 749, 739 cm⁻¹. HRMS Calcd for C₁₆H₁₃N₄O₄ *m/z*: 325.0937 (M-H)⁻, found 325.0931. HPLC: *t_r* = 14.37 min (100.0% at 254 nm).

4.3.12 Ethyl 5-(3-(4-bromo-1H-pyrrole-2-carboxamido)phenyl)-1,2,4-oxadiazole-3-carboxylate (12). Synthesized according to the general procedure for acidolytic cleavage of

Boc protecting groups and the subsequent TBTU-mediated coupling. Beige amorphous powder; m.p. 254-256 °C. ¹H-NMR (DMSO-d₆, 400 MHz): δ = 1.36 (t, 3H, *J* = 7.2 Hz, -CH₂-CH₃), 4.45 (q, 2H, *J* = 7.2 Hz, -CH₂-CH₃), 7.15-7.16 (m, 1H, Ar-H), 7.22-7.23 (m, 1H, Ar-H), 7.63 (t, 1H, *J* = 8.0 Hz, Ar-H), 7.84-7.86 (m, 1H, Ar-H), 8.14-8.16 (m, 1H, Ar-H), 8.62 (t, 1H, *J* = 2.0 Hz, Ar-H), 10.15 (s, 1H, -CONH), 12.14 (s, 1H, pyrrole-NH) ppm. ¹³C-NMR (DMSO-d₆, 100 MHz): δ = 13.88, 62.59, 83.66, 95.36, 113.17, 118.67, 122.47, 122.95, 124.34, 130.26, 140.19, 144.20, 158.29, 162.12, 163.29, 176.45 ppm. MS (ESI): *m/z* (%) = 403.0 (M-H)⁻. IR (KBr): ν = 3395, 3241, 3135, 2922, 1726, 1658, 1600, 1559, 1529, 1490, 1431, 1404, 1377, 1353, 1330, 1292, 1261, 1223, 1169, 1138, 1097, 1078, 1024, 919, 891, 874, 826, 800, 792, 760, 740, 680, 602 cm⁻¹. HRMS Calcd for C₁₆H₁₂BrN₄O₄ *m/z*: 403.0042 (M-H)⁻, found 403.0049. HPLC: *t_r* = 18.76 min (97.3% at 254 nm).

4.3.13 Ethyl 5-(3-(4,5-dibromo-1H-pyrrole-2-carboxamido)phenyl)-1,2,4-oxadiazole-3-carboxylate (13). Synthesized according to the general procedure for acidolytic cleavage of Boc protecting groups and the subsequent TBTU-mediated coupling. Beige amorphous powder; m.p. 265-267 °C. ¹H-NMR (DMSO-d₆, 400 MHz): δ = 1.37 (t, 3H, *J* = 7.2 Hz, -CH₂-CH₃), 4.46 (q, 2H, *J* = 7.2 Hz, -CH₂-CH₃), 7.30 (s, 1H, Ar-H), 7.65 (t, 1H, *J* = 8.0 Hz, Ar-H), 7.87 (dd, 1H, *J* = 8.4 Hz, *J* = 1.6 Hz, Ar-H), 8.14 (dd, 1H, *J* = 8.4 Hz, *J* = 1.2 Hz, Ar-H), 8.61 (d, 1H, *J* = 2.0 Hz, Ar-H), 10.18 (s, 1H, -CONH), 13.02 (s, 1H, pyrrole-NH) ppm. ¹³C-NMR (DMSO-d₆, 100 MHz): δ = 13.87, 62.59, 106.60, 114.25, 118.69, 118.89, 122.59, 123.13, 124.36, 127.49, 130.30, 140.01, 157.16, 157.54, 162.12, 176.41 ppm. MS (ESI): *m/z* (%) = 482.9 (M+H)⁺. IR (KBr): ν = 3398, 3284, 3195, 1731, 1695, 1664, 1593, 1525, 1488, 1437, 1413, 1376, 1350, 1327, 1297, 1272, 1220, 1113, 1078, 741, 676 cm⁻¹. HRMS Calcd for C₁₆H₁₃Br₂N₄O₄ *m/z*: 482.9304 (M+H)⁺, found 482.9300. HPLC: *t_r* = 20.32 min (94.9% at 254 nm).

4.3.14 Ethyl 5-(3-(1H-indole-2-carboxamido)phenyl)-1,2,4-oxadiazole-3-carboxylate (14).

Synthesized according to the general procedure for acidolytic cleavage of Boc protecting groups and the subsequent TBTU-mediated coupling. Yellow amorphous powder; m.p. 179-182 °C. ¹H-NMR (DMSO-d₆, 400 MHz): δ = 1.37 (t, 3H, *J* = 7.2 Hz, -CH₂-CH₃), 4.46 (q, 2H, *J* = 7.2 Hz, -CH₂-CH₃), 7.09 (t, 1H, *J* = 8.0 Hz, Ar-H), 7.25 (t, 1H, *J* = 8.0 Hz, Ar-H), 7.47-7.50 (m, 2H, Ar-H), 7.65-7.72 (m, 2H, Ar-H), 7.88-7.91 (m, 1H, Ar-H), 8.23-8.26 (m, 1H, Ar-H), 8.71 (t, 1H, *J* = 2.0 Hz, Ar-H), 10.55 (s, 1H, -CONH), 11.81 (s, 1H, indole-NH) ppm. ¹³C-NMR (DMSO-d₆, 100 MHz): δ = 13.88, 62.60, 104.37, 112.43, 118.89, 120.03, 121.88, 122.71, 123.15, 124.06, 124.59, 126.95, 130.30, 130.92, 136.96, 140.12, 157.18, 160.02, 162.14, 176.45 ppm. MS (ESI): *m/z* (%) = 375.1 (M-H)⁻. IR (KBr): ν = 3517, 3448, 3121, 2981, 1735, 1653, 1573, 1540, 1478, 1445, 1412, 1314, 1240, 1212, 1108, 1029, 740, 680, 633 cm⁻¹. HRMS Calcd for C₂₀H₁₅N₄O₄ *m/z*: 375.1093 (M-H)⁻, found 375.1090. HPLC: *t_r* = 20.44 min (95.5% at 254 nm).

4.3.15 Ethyl 5-(3-(5-fluoro-1H-indole-2-carboxamido)phenyl)-1,2,4-oxadiazole-3-carboxylate (15).

Synthesized according to the general procedure for acidolytic cleavage of Boc protecting groups and the subsequent TBTU-mediated coupling. Yellow amorphous powder; m.p. 230-232 °C. ¹H-NMR (DMSO-d₆, 400 MHz): δ = 1.38 (t, 3H, *J* = 7.2 Hz, -CH₂-CH₃), 4.47 (q, 2H, *J* = 7.2 Hz, -CH₂-CH₃), 7.13 (dt, 1H, *J* = 9.2 Hz, *J* = 2.4 Hz, Ar-H), 7.48-7.53 (m, 3H, Ar-H), 7.69 (t, 1H, *J* = 8.0 Hz, Ar-H), 7.91 (dd, 1H, *J* = 8.0 Hz, *J* = 1.2 Hz, Ar-H), 8.24 (dd, 1H, *J* = 8.0 Hz, *J* = 2.0 Hz, Ar-H), 8.71 (t, 1H, *J* = 2.0 Hz, Ar-H), 10.60 (s, 1H, -CONH), 11.93 (s, 1H, indole-NH) ppm. MS (ESI): *m/z* (%) = 393.1 (M-H)⁻. IR (KBr): ν = 3395, 3297, 1727, 1658, 1560, 1538, 1489, 1449, 1402, 1380, 1357, 1290, 1226, 1144, 1110, 1027, 798, 757, 741, 732 cm⁻¹. HRMS Calcd for C₂₀H₁₄FN₄O₄ *m/z*: 393.0999 (M-H)⁻, found 393.1010. HPLC: *t_r* = 21.22 min (97.3% at 254 nm).

4.3.16 5-(3-(1H-pyrrole-2-carboxamido)phenyl)-1,2,4-oxadiazole-3-carboxylic acid (16).

Synthesized according to the general procedure for alkaline hydrolysis described in [41]. Beige amorphous powder; m.p. 207-210 °C. ¹H-NMR (DMSO-d₆, 400 MHz): δ = 6.19-6.20 (m, 1H, Ar-H), 7.01 (s, 1H, Ar-H), 7.13 (s, 1H, Ar-H), 7.61 (t, 1H, *J* = 8.0 Hz, Ar-H), 7.82 (d, 1H, *J* = 8.0 Hz, Ar-H), 8.15 (dd, 1H, *J* = 8.0 Hz, *J* = 1.2 Hz, Ar-H), 8.63 (s, 1H, Ar-H), 10.08 (s, 1H, -CONH), 11.74 (s, 1H, pyrrole-NH) ppm. ¹³C-NMR (DMSO-d₆, 100 MHz): δ = 109.08, 111.82, 118.58, 122.10, 123.11, 123.20, 124.23, 125.58, 130.10, 140.50, 158.57, 159.33, 162.91, 176.31 ppm. MS (ESI): *m/z* (%) = 297.1 (M-H)⁻. IR (KBr): ν = 3375, 3320, 2924, 1712, 1624, 1597, 1574, 1547, 1531, 1509, 1484, 1420, 1337, 1224, 1166, 1127, 1082, 1054, 999, 891, 762, 739, 679, 637 cm⁻¹. HRMS Calcd for C₁₄H₉N₄O₄ *m/z*: 297.0624 (M-H)⁻, found 297.0630. HPLC: *t_r* = 5.56 min (99.7% at 254 nm).

4.3.17 5-(3-(4-Bromo-1H-pyrrole-2-carboxamido)phenyl)-1,2,4-oxadiazole-3-carboxylic acid (17). Synthesized according to the general procedure for alkaline hydrolysis described in [41].

Beige amorphous powder; m.p. 140-144 °C. ¹H-NMR (DMSO-d₆, 400 MHz): δ = 7.12-7.13 (m, 1H, Ar-H), 7.19-7.20 (m, 1H, Ar-H), 7.48 (t, 1H, *J* = 8.0 Hz, Ar-H), 7.58 (dt, 1H, *J* = 7.6 Hz, *J* = 1.2 Hz, Ar-H), 8.02 (dd, 1H, *J* = 8.0 Hz, *J* = 1.6 Hz, Ar-H), 8.26 (t, 1H, *J* = 2.0 Hz, Ar-H), 10.04 (s, 1H, -CONH), 12.09 (s, 1H, pyrrole-NH) ppm. ¹³C-NMR (DMSO-d₆, 100 MHz): δ = 95.30, 113.01, 115.93, 119.68, 119.76, 122.71, 124.19, 126.28, 129.02, 139.41, 158.16, 163.88, 164.96, 170.70 ppm. MS (ESI): *m/z* (%) = 375.0 (M-H)⁻. IR (KBr): ν = 3260, 2960, 2920, 1721, 1656, 1572, 1553, 1532, 1477, 1444, 1379, 1334, 1296, 1261, 1220, 1134, 1094, 1016, 794, 742, 678 cm⁻¹. HRMS Calcd for C₁₄H₈BrN₄O₄ *m/z*: 374.9729 (M-H)⁻, found 374.9720. HPLC: *t_r* = 9.98 min (95.5% at 254 nm).

4.3.18 5-(3-(4,5-Dibromo-1H-pyrrole-2-carboxamido)phenyl)-1,2,4-oxadiazole-3-carboxylic acid (18). Synthesized according to the general procedure for alkaline hydrolysis described in [41]. Beige amorphous powder; m.p. 156-160 °C. ¹H-NMR (DMSO-d₆, 400 MHz): δ = 7.27 (d, 1H, *J* = 2.8 Hz, Ar-H), 7.51 (t, 1H, *J* = 8.0 Hz, Ar-H), 7.59-7.61 (m, 1H, Ar-H), 8.02-8.04 (m, 1H, Ar-H), 8.26 (s, 1H, Ar-H), 10.10 (s, 1H, -CONH), 12.97 (s, 1H, pyrrole-NH) ppm. ¹³C-NMR (DMSO-d₆, 100 MHz): δ = 98.27, 102.97, 106.36, 114.15, 119.67, 122.78, 124.44, 127.54, 129.19, 131.41, 139.35, 148.64, 157.43, 174.77 ppm. MS (ESI): *m/z* (%) = 454.9 (M+H)⁺. IR (KBr): ν = 3206, 2964, 1725, 1636, 1573, 1555, 1539, 1477, 1420, 1386, 1337, 1304, 1214, 742, 679 cm⁻¹. HRMS Calcd for C₁₄H₉Br₂N₄O₄ *m/z*: 454.8991 (M+H)⁺, found 454.8998. HPLC: *t_r* = 12.91 min (94.3% at 254 nm).

4.3.19 5-(3-(1H-indole-2-carboxamido)phenyl)-1,2,4-oxadiazole-3-carboxylic acid (19). Synthesized according to the general procedure for alkaline hydrolysis described in [41]. Beige amorphous powder; m.p. 176-180 °C. ¹H-NMR (DMSO-d₆, 400 MHz): δ = 7.07 (t, 1H, *J* = 7.6 Hz, Ar-H), 7.23 (t, 1H, *J* = 7.6 Hz, Ar-H), 7.44-7.53 (m, 3H, Ar-H), 7.63-7.69 (m, 2H, Ar-H), 8.11 (dd, 1H, *J* = 8.8 Hz, *J* = 1.2 Hz, Ar-H), 8.35-8.45 (m, 1H, Ar-H), 10.45 (s, 1H, -CONH), 11.78 (s, 1H, indole-NH) ppm. ¹³C-NMR (DMSO-d₆, 100 MHz): δ = 104.21, 112.39, 119.95, 120.76, 121.83, 122.98, 123.91, 124.23, 126.98, 128.95, 128.98, 131.10, 136.88, 139.29, 148.92, 159.85, 167.17, 174.89 ppm. MS (ESI): *m/z* (%) = 349.1 (M+H)⁺. IR (KBr): ν = 3283, 3197, 2963, 2920, 1651, 1611, 1590, 1538, 1476, 1440, 1414, 1228, 1193, 1144, 1107, 741, 679 cm⁻¹. HRMS Calcd for C₁₈H₁₃N₄O₄ *m/z*: 349.0937 (M+H)⁺, found 349.0938. HPLC: *t_r* = 11.81 min (98.3% at 254 nm).

4.3.20 5-(3-(5-Fluoro-1H-indole-2-carboxamido)phenyl)-1,2,4-oxadiazole-3-carboxylic acid (20). Synthesized according to the general procedure for alkaline hydrolysis described in [41].

Beige amorphous powder; m.p. 240-243 °C. ¹H-NMR (DMSO-d₆, 400 MHz): δ = 7.07-7.12 (m, 1H, Ar-H), 7.41-7.47 (m, 4H, Ar-H), 7.66 (d, 1H, *J* = 7.6 Hz, Ar-H), 8.08 (d, 1H, *J* = 7.6 Hz, Ar-H), 8.32 (s, 1H, Ar-H), 10.45 (s, 1H, -CONH), 11.89 (s, 1H, indole-NH) ppm. MS (ESI): *m/z* (%) = 321.1 (M-H-CO₂)⁻. IR (KBr): ν = 3397, 3299, 1662, 1540, 1477, 1446, 1413, 1330, 1293, 1203, 1147, 1109, 795, 742, 676 cm⁻¹. Anal. Calcd for C₁₈H₁₁FN₄O₄ × 1.7 H₂O (%): C, 54.47; H, 3.66; N, 14.11. Found: C, 54.52; H, 3.46; N, 13.93. HPLC: *t_r* = 12.81 min (93.3% at 254 nm).

4.3.21 Ethyl 5-(3-(1H-indole-2-carboxamido)phenyl)-1,3,4-oxadiazole-2-carboxylate (22).

Synthesized as described in [42]. Yellow amorphous powder; m.p. 225-227 °C. ¹H-NMR (DMSO-d₆, 400 MHz): δ = 1.39 (t, 3H, *J* = 7.2 Hz, -CH₂-CH₃), 4.48 (q, 2H, *J* = 7.2 Hz, -CH₂-CH₃), 7.09 (t, 1H, *J* = 8.0 Hz, Ar-H), 7.25 (t, 1H, *J* = 8.0 Hz, Ar-H), 7.48-7.51 (m, 2H, Ar-H), 7.65 (t, 1H, *J* = 8.0 Hz, Ar-H), 7.71 (d, 1H, *J* = 8.4 Hz, Ar-H), 7.82 (d, 1H, *J* = 8.8 Hz, Ar-H), 8.21 (dd, 1H, *J* = 8.0 Hz, *J* = 2.0 Hz, Ar-H), 8.60-8.61 (m, 1H, Ar-H), 10.55 (s, 1H, -CONH), 11.81 (s, 1H, indole-NH) ppm. ¹³C-NMR (DMSO-d₆, 100 MHz): δ = 13.89, 62.91, 104.34, 112.42, 117.94, 120.00, 121.87, 121.90, 122.96, 123.72, 124.02, 126.96, 130.20, 130.98, 136.94, 140.10, 154.04, 156.51, 160.01, 165.29 ppm. MS (ESI): *m/z* (%) = 377.1 (M+H)⁺. IR (KBr): ν = 3348, 3311, 3123, 3060, 2985, 1749, 1698, 1677, 1650, 1603, 1557, 1530, 1492, 1475, 1455, 1404, 1383, 1365, 1352, 1316, 1289, 1229, 1203, 1167, 1103, 1082, 1028, 968, 899, 872, 861, 838, 824, 800, 767, 746, 729, 684, 641, 613, 571, 555 cm⁻¹. HRMS Calcd for C₂₀H₁₇N₄O₄ *m/z*: 377.1250 (M+H)⁺, found 377.1260. HPLC: *t_r* = 17.16 min (100% at 254 nm).

4.3.22 N-(3-(1,3,4-oxadiazol-2-yl)phenyl)-1H-indole-2-carboxamide (23). Synthesized according to the general procedure for alkaline hydrolysis described in [41]. Grey amorphous powder; m.p. 238-240 °C. ¹H-NMR (DMSO-d₆, 400 MHz): δ = 7.09 (t, 1H, *J* = 8.0 Hz, Ar-

H), 7.24 (t, 1H, $J = 8.0$ Hz, Ar-H), 7.48-7.50 (m, 2H, Ar-H), 7.62 (t, 1H, $J = 7.6$ Hz, Ar-H), 7.70 (d, 1H, $J = 7.2$ Hz, Ar-H), 7.76 (d, 1H, $J = 8.0$ Hz, Ar-H), 8.12 (s, 1H, Ar-H), 8.59 (s, 1H, Ar-H), 9.38 (s, 1H, Ar-H), 10.51 (s, 1H, -CONH), 11.80 (s, 1H, indole-NH) ppm. MS (ESI): m/z (%) = 303.1 (M-H)⁻. IR (KBr): $\nu = 3296, 2331, 2016, 1656, 1569, 1538, 1474, 1445, 1417, 1329, 1311, 1242, 1191, 1146, 1117, 1086, 961, 896, 872, 793, 731, 681, 638, 610, 602, 577, 565, 555$ cm⁻¹. HRMS Calcd for C₁₇H₁₁N₄O₂ m/z : 303.0882 (M-H)⁻, found 303.0877. HPLC: t_r = 11.44 min (96.4% at 254 nm).

4.3.23 5-(3-(1H-indole-2-carboxamido)phenyl)-1,3,4-oxadiazole-2-carboxamide (24).

Synthesized according to the general procedure for aminolysis described in [40]. White amorphous powder; m.p. 264-268 °C. ¹H-NMR (DMSO-d₆, 400 MHz): $\delta = 7.09$ (t, 1H, $J = 7.6$ Hz, Ar-H), 7.25 (t, 1H, $J = 8.0$ Hz, Ar-H), 7.48-7.50 (m, 2H, Ar-H), 7.71 (d, 1H, $J = 8.0$ Hz, Ar-H), 7.81 (d, 1H, $J = 8.0$ Hz, Ar-H), 8.17 (dd, 1H, $J = 8.0$ Hz, $J = 2.0$ Hz, Ar-H), 8.28 (s, 1H, CONH₂), 8.61 (t, 1H, $J = 1.6$ Hz, Ar-H), 8.71 (s, 1H, CONH₂), 10.54 (s, 1H, -CONH), 11.81 (s, 1H, indole-NH) ppm. ¹³C-NMR (DMSO-d₆, 100 MHz): $\delta = 104.30, 112.42, 118.00, 120.00, 121.87, 123.24, 124.01, 126.97, 130.10, 131.00, 136.93, 139.99, 153.41, 154.54, 158.62, 159.98, 165.00, 167.33$ ppm. MS (ESI): m/z (%) = 346.1 (M-H)⁻. IR (KBr): $\nu = 3307, 3193, 2926, 2359, 2162, 1987, 1957, 1702, 1651, 1597, 1565, 1531, 1419, 1341, 1312, 1279, 1238, 1190, 1145, 1105, 1079, 999, 885, 852, 793, 740, 707, 677, 623, 616, 601, 591, 574, 561, 553$ cm⁻¹. HRMS Calcd for C₁₈H₁₂N₅O₃ m/z : 346.0940 (M-H)⁻, found 346.0949. HPLC: t_r = 9.98 min (100.0% at 254 nm).

4.3.24 5-(3-(1H-indole-2-carboxamido)phenyl)-1,2,4-oxadiazole-3-carboxamide (25).

Synthesized according to the general procedure for aminolysis described in [40]. White amorphous powder; m.p. 288-290 °C. ¹H-NMR (DMSO-d₆, 400 MHz): $\delta = 7.10$ (t, 1H, $J =$

7.2 Hz, Ar-H), 7.26 (t, 1H, $J = 7.2$ Hz, Ar-H), 7.49-7.51 (m, 2H, Ar-H), 7.66-7.73 (m, 2H, Ar-H), 7.90 (dd, 1H, $J = 7.6$ Hz, $J = 1.2$ Hz, Ar-H), 8.17-8.20 (m, 2H, Ar-H, CONH₂), 8.44 (s, 1H, CONH₂), 8.71 (t, 1H, $J = 2.0$ Hz, Ar-H), 10.57 (s, 1H, -CO-NH-), 11.81 (s, 1H, indole-NH) ppm. ¹³C-NMR (DMSO-d₆, 100 MHz): $\delta = 104.39, 112.43, 118.90, 120.03, 121.88, 122.83, 124.06, 124.57, 126.95, 130.23, 130.93, 136.95, 140.03, 147.64, 157.77, 160.02, 164.39, 175.86$ ppm. MS (ESI): m/z (%) = 346.1 (M-H)⁻. IR (KBr): $\nu = 3471, 3355, 3301, 3117, 1690, 1655, 1619, 1598, 1566, 1540, 1491, 1445, 1399, 1317, 1272, 1229, 1201, 1150, 735, 680, 642$ cm⁻¹. HRMS Calcd for C₁₈H₁₂N₅O₄ m/z : 346.0940 (M-H)⁻, found 346.0945. HPLC: $t_r = 11.23$ min (100.0% at 254 nm).

4.3.25 5-(3-(1H-indole-2-carboxamido)phenyl)-N-hydroxy-1,2,4-oxadiazole-3-carboxamide (26). Synthesized according to the procedure described in [40]. White amorphous powder; m.p. 187-190 °C. ¹H-NMR (DMSO-d₆, 400 MHz): $\delta = 7.10$ (t, 1H, $J = 7.6$ Hz, Ar-H), 7.26 (t, 1H, $J = 8.0$ Hz, Ar-H), 7.49-7.52 (m, 2H, Ar-H), 7.67 (d, 1H, $J = 7.6$ Hz, Ar-H), 7.71 (d, 1H, $J = 8.4$ Hz, Ar-H), 7.89 (d, 1H, $J = 8.0$ Hz, Ar-H), 8.20 (dd, 1H, $J = 9.6$ Hz, $J = 1.2$ Hz, Ar-H), 8.73 (s, 1H, Ar-H), 10.23 (s, 1H, -NH-OH), 10.63 (s, 1H, -CO-NH-), 11.85 (s, 1H, indole-NH), 11.96 (s, 1H, -NH-OH) ppm. ¹³C-NMR (DMSO-d₆, 100 MHz): $\delta = 104.52, 112.43, 118.93, 120.02, 121.87, 122.85, 123.26, 124.05, 124.66, 126.94, 130.22, 130.95, 136.95, 140.07, 153.58, 160.00, 163.27, 175.82$ ppm. MS (ESI): m/z (%) = 362.1 (M-H)⁻. IR (KBr): $\nu = 3396, 3348, 3185, 1640, 1618, 1568, 1533, 1475, 1440, 1413, 1364, 1326, 1311, 1244, 746$ cm⁻¹. HRMS Calcd for C₁₈H₁₂N₅O₄ m/z : 362.0889 (M-H)⁻, found 362.0883. HPLC: $t_r = 9.50$ min (82.5% at 254 nm).

4.3.26 Ethyl 5-(4-(1H-indole-2-carboxamido)benzyl)-1,2,4-oxadiazole-3-carboxylate (28). Synthesized according to the general procedure for acidolytic cleavage of Boc protecting

groups and the subsequent TBTU-mediated coupling. Beige solid; m.p. 189-193 °C. ¹H-NMR (DMSO-d₆, 400 MHz): δ = 1.31 (t, 3H, *J* = 7.2 Hz, -CH₂-CH₃), 4.39 (q, 2H, *J* = 7.2 Hz, -CH₂-CH₃), 4.43 (s, 2H, Ar-CH₂), 7.07 (t, 1H, *J* = 8.0 Hz, Ar-H), 7.22 (dt, 1H, *J* = 8.0 Hz, *J* = 1.2 Hz, Ar-H), 7.36 (d, 2H, *J* = 8.8 Hz, Ar-H), 7.43-7.47 (m, 2H, Ar-H), 7.68 (d, 1H, *J* = 8.0 Hz, Ar-H), 7.81 (d, 2H, *J* = 8.4 Hz, Ar-H), 10.29 (s, 1H, -CONH), 11.78 (s, 1H, NH) ppm. ¹³C-NMR (DMSO-d₆, 100 MHz): δ = 13.83, 31.39, 62.47, 103.96, 112.36, 119.90, 120.38, 121.73, 123.78, 126.97, 128.48, 129.51, 131.35, 136.80, 138.27, 157.17, 159.70, 161.61, 180.43 ppm. MS (ESI): *m/z* (%) = 389.1 (M-H)⁻. IR (KBr): ν = 3275, 2932, 1692, 1600, 1529, 1374, 1341, 1308, 1233, 1198, 1147, 1090, 968, 780, 740 cm⁻¹. HRMS Calcd for C₂₁H₁₈N₄O₄ *m/z*: 389.1250 (M-H)⁻, found 389.1255. HPLC: *t_r* = 18.17 min (95.6% at 254 nm).

4.3.27 Ethyl 5-(4-(4,5-dibromo-1H-pyrrole-2-carboxamido)benzyl)-1,2,4-oxadiazole-3-carboxylate (29). Synthesized according to the general procedure for acidolytic cleavage of Boc protecting groups and the subsequent TBTU-mediated coupling. Ochre solid; m.p. 185-187 °C. ¹H-NMR (DMSO-d₆, 400 MHz): δ = 1.32 (t, 3H, *J* = 7.2 Hz, -CH₂-CH₃), 4.37-4.42 (m, 4H, -CH₂-CH₃ and Ar-CH₂), 7.25 (s, 1H, Ar-H), 7.33 (d, 1H, *J* = 8.8 Hz, Ar-H), 7.69-7.73 (m, 2H, Ar-H), 9.96 (s, 1H, -CONH), 12.96 (s, 1H, NH) ppm. ¹³C-NMR (DMSO-d₆, 100 MHz): δ = 13.82, 31.36, 62.47, 98.15, 105.87, 113.99, 120.19, 127.82, 129.48, 138.13, 142.42, 157.16, 157.26, 161.59, 180.42 ppm. MS (ESI): *m/z* (%) = 494.9 (M-H)⁻. IR (KBr): ν = 3399, 3323, 1651, 1596, 1519, 1448, 1408, 1341, 1317, 1222, 1189, 1142, 799, 742, 639 cm⁻¹. HRMS Calcd for C₁₇H₁₃Br₂N₄O₄ *m/z*: 494.9309 (M-H)⁻, found 494.9312. HPLC: *t_r* = 19.08 min (94.8% at 254 nm).

4.3.28 5-(4-(1H-indole-2-carboxamido)benzyl)-1,2,4-oxadiazole-3-carboxylic acid (30).

Synthesized according to the general procedure for alkaline hydrolysis described in [41]. Beige solid; m.p. 221-223 °C. ¹H-NMR (DMSO-d₆, 400 MHz): δ = 3.67 (s, 2H, Ar-CH₂), 7.05-7.09 (m, 2H, Ar-H), 7.21-7.27 (m, 3H, Ar-H), 7.42-7.48 (m, 2H, Ar-H), 7.63-7.77 (m, 2H, Ar-H), 10.24 (s, 1H, -CONH), 11.75 (s, 1H, NH), 12.89 (s, 1H, COOH) ppm. ¹³C-NMR (DMSO-d₆, 100 MHz): δ = 30.67, 103.85, 107.26, 112.45, 119.92, 120.16, 121.91, 124.24, 126.99, 128.36, 129.72, 131.40, 136.79, 137.90, 159.67, 162.79, 172.08 ppm. MS (ESI): m/z (%) = 363.1 (M+H)⁺. IR (KBr): ν = 3401, 1650, 1596, 1533, 1448, 1408, 1341, 1317, 1223, 1189, 1146, 799, 742, 640 cm⁻¹. HRMS Calcd for C₁₉H₁₅N₄O₄ m/z: 363.1093 (M+H)⁺, found 363.1095. HPLC: t_r = 11.40 min (93.9% at 254 nm).

4.3.29 5-(4-(4,5-Dibromo-1H-pyrrole-2-carboxamido)benzyl)-1,2,4-oxadiazole-3-carboxylic acid (31).

Synthesized according to the general procedure for alkaline hydrolysis described in [41]. Beige solid; m.p. 218-220 °C. ¹H-NMR (MeOD, 400 MHz): δ = 3.67 (s, 2H, Ar-CH₂), 7.07 (s, 1H, Ar-H), 7.25 (d, 2H, J = 8.0 Hz, Ar-H), 7.64 (d, 2H, J = 8.0 Hz, Ar-H) ppm. ¹³C-NMR (MeOD, 100 MHz): δ = 42.17, 100.23, 107.00, 115.10, 118.64, 122.06, 128.98, 130.20, 130.82, 139.03, 159.78, 164.63, 173.69 ppm. MS (ESI): m/z (%) = 468.9 (M+H)⁺. IR (KBr): ν = 3397, 2917, 2849, 1687, 1651, 1516, 1449, 1369, 1319, 1244, 1174, 1145, 1070, 1011, 976, 927, 853, 800, 749, 608 cm⁻¹. HRMS Calcd for C₁₅H₁₁Br₂N₄O₄ m/z: 468.9147 (M+H)⁺, found 468.9140. HPLC: t_r = 12.49 min (94.8% at 254 nm).

4.3.30 Ethyl 5-((4-aminophenyl)amino)-1,2,4-oxadiazole-3-carboxylate (33).

Synthesized from **46** according to the procedure for nucleophilic displacement described in [44]. Brown solidified oil; m.p. /. ¹H-NMR (DMSO-d₆, 400 MHz): δ = 1.29 (t, 3H, J = 7.2 Hz, -CH₂-CH₃), 4.35 (q, 2H, J = 7.2 Hz, -CH₂-CH₃) 5.05 (s, 2H, NH₂), 6.58 (d, 2H, J = 8.8 Hz, Ar-H), 7.15 (d,

2H, $J = 8.4$ Hz, Ar-H), 10.72 (s, 1H, NH) ppm. ^{13}C -NMR (DMSO- d_6 , 100 MHz): $\delta = 14.37$, 62.60, 120.95, 128.53, 133.19, 138.93, 139.44, 158.41, 169.79 ppm. MS (ESI): m/z (%) = 249.9 (M+H) $^+$. IR (KBr): $\nu = 2983$, 1736, 1628, 1592, 1512, 1412, 1385, 1202, 831, 733, 626 cm^{-1} . HRMS Calcd for $\text{C}_{11}\text{H}_{12}\text{N}_4\text{O}_3$ m/z : 249.0988 (M+H) $^+$, found 249.0988.

4.3.31 5-((4-(4,5-Dibromo-1H-pyrrole-2-carboxamido)phenyl)amino)-1,2,4-oxadiazole-3-carboxylic acid (**34**). To a stirred solution of 4,5-dibromo-pyrrole-2-carboxylic acid (1.0 eq) in dry dichloromethane (10 mL), diisopropylethylamine (3.0 eq) and TBTU (1.1 eq) were added. After stirring for 45 minutes the amine **33** was added at 0 $^{\circ}\text{C}$, and the mixture allowed to warm to room temperature; stirring then continued for 48 h. On completion, the reaction mixture was diluted with dichloromethane (30 mL) then washed with 1M HCl (2×20 mL), water (20 mL), saturated NaHCO_3 solution (2×20 mL), water (20 mL) and dried over anhydrous Na_2SO_4 . The solvent was concentrated in vacuo and the residue of crude ester immediately used in the next step. The crude ester (1.0 eq) was dissolved in THF, then 1M NaOH (1.1 eq) was added and the reaction mixture stirred at room temperature for 2 h. THF was evaporated under vacuum and the resulting aqueous solution neutralized with 1M HCl until the product **34** precipitated. It was then dried overnight. Brown solid; m.p. 200-203 $^{\circ}\text{C}$. ^1H -NMR (DMSO- d_6 , 400 MHz): $\delta = 7.19$ (s, 1H, Ar-H), 7.41 (d, 2H, $J = 8.8$ Hz, Ar-H), 7.55 (d, 2H, $J = 8.8$ Hz, Ar-H), 8.99 (s, 1H, Ar-NH), 9.77 (s, 1H, CONH), 12.87 (s, 1H, NH) ppm. ^{13}C -NMR (DMSO- d_6 , 100 MHz): $\delta = 99.03$, 106.17, 113.49, 117.18, 120.97, 124.64, 125.26, 127.59, 139.83, 160.97, 160.98, 185.55 ppm. MS (ESI): m/z (%) = 423.9 (M-H- CO_2) $^-$. IR (KBr): $\nu = 3394$, 3322, 1651, 1597, 1515, 1448, 1408, 1372, 1342, 1318, 1223, 1189, 1143, 800, 740, 630 cm^{-1} . HRMS Calcd for $\text{C}_{13}\text{H}_8\text{Br}_2\text{N}_5\text{O}_2$ m/z : 423.9045 (M+H) $^+$, found 423.9034. HPLC: $t_r = 10.85$ min (94.6% at 254 nm).

4.3.32 5-((4-(3,4-dichloro-5-methyl-1H-pyrrole-2-carboxamido)phenyl)amino)-1,2,4-oxadiazole-3-carboxylic acid (**35**). To a stirred solution of 3,4-dichloro-5-methyl-pyrrole-2-carboxylic acid (1.0 eq) in dry dichloromethane (10 mL), diisopropylethylamine (3.0 eq) and TBTU (1.1 eq) were added. After stirring for 45 minutes the amine **33** was added at 0 °C, and the mixture allowed to warm to room temperature; stirring then continued for 48 h. On completion, the reaction mixture was diluted with dichloromethane (30 mL) then washed with 1M HCl (2 × 20 mL), water (20 mL), saturated NaHCO₃ solution (2 × 20 mL), water (20 mL) and dried over anhydrous Na₂SO₄. The solvent was concentrated in vacuo and the residue of crude ester immediately used in the next step. The crude ester (1.0 eq) was dissolved in THF, then 1M NaOH (1.1 eq) was added and the reaction mixture stirred at room temperature for 2 h. THF was evaporated under vacuum and the resulting aqueous solution neutralized with 1M HCl until the product **35** precipitated. It was then dried overnight. Brown solid; m.p. 176-180 °C. ¹H-NMR (DMSO-d₆, 400 MHz): δ = 2.22 (s, 3H, Ar-CH₃), 7.40 (d, 2H, *J* = 8.8 Hz, Ar-H), 7.57 (d, 2H, *J* = 8.8 Hz, Ar-H), 9.35 (s, 1H, Ar-NH), 9.36 (s, 1H, CONH), 12.14 (s, 1H, NH) ppm. ¹³C-NMR (DMSO-d₆, 100 MHz): δ = 10.75, 108.28, 110.89, 119.63, 119.67, 120.48, 127.81, 133.80, 134.31, 151.96, 157.00, 180.65 ppm. MS (ESI): *m/z* (%) = 350.0 (M-H-CO₂)⁻. IR (KBr): ν = 3394, 3321, 1651, 1598, 1515, 1449, 1409, 1373, 1317, 1249, 1190, 1130, 1045, 960, 800, 738, 627 cm⁻¹. HRMS Calcd for C₁₄H₁₀Cl₂N₅O₂ *m/z*: 350.0212 (M+H)⁺, found 350.0217. HPLC: *t_r* = 12.44 min (97.2% at 254 nm).

4.4 In vitro Inhibitory Activity Screening and Determination of IC₅₀ Values on *E. coli* and *S. aureus* Gyrase. The assay for determining IC₅₀ values (Inspiralis) was performed on black streptavidin-coated 96-well microtiter plates (Thermo Scientific Pierce). The plate was first rehydrated with the wash buffer supplied (20 mM Tris-HCl (pH 7.6), 137 mM NaCl, 0.01% (w/v) BSA, 0.05% (v/v) Tween 20). Biotinylated oligonucleotide was immobilized

onto the wells. The excess of oligonucleotide was then washed off and the enzyme assay carried out in the wells. The final reaction volume of 30 μ L in buffer (35 mM Tris HCl pH 7.5; 24 mM KCl; 4 mM MgCl₂; 2 mM DTT; 1.8 mM spermidine; 1 mM ATP; 6.5 % (w/v) glycerol; 0.1 mg/mL albumin) contained 1.5 U of DNA gyrase from *E. coli* or *S. aureus*, 0.75 μ g of relaxed pNO1 plasmid, and 3 μ L of inhibitors solution in 10% DMSO and 0.008% Tween[®] 20. Reactions were incubated for 30 min at 37 °C and, after addition of the TF buffer (50 mM NaOAc pH 5.0, 50 mM NaCl and 50 mM MgCl₂), which terminated the enzymatic reaction, for another 30 min at room temperature to allow triplex formation (biotin–oligonucleotide–plasmid). The unbound plasmid was then washed off using TF buffer, and a solution of SybrGOLD stain in T10 buffer (10 mM Tris \times HCl pH 8.0 and 1 mM EDTA) was added. After mixing, the fluorescence (excitation, 485 nm; emission, 535 nm) was read using a BioTek's Synergy H4 microplate reader. Preliminary screening was performed at inhibitor concentrations of 100 μ M and 10 μ M. For the most potent compounds IC₅₀ was determined with 7 concentrations of the inhibitors. IC₅₀ values were calculated using GraphPad Prism software and represent the concentration of inhibitor where the residual activity of the enzyme is 50% in three independent measurements; the final result is given as their average value. Novobiocin (IC₅₀ = 0.17 μ M (lit. 0.08 μ M [45]) for *E. coli* DNA gyrase and IC₅₀ = 0.041 μ M (lit. 0.01 μ M [45]) for *S. aureus* DNA gyrase) was used as a positive control.

4.5 *In vitro* Inhibitory Activity Screening and Determination of IC₅₀ Values on *E. coli* and *S. aureus* topoisomerase IV. The assay for the determination of IC₅₀ values (Inspiralis) was performed on the black streptavidin-coated 96-well microtiter plates (Thermo Scientific Pierce). The plate was first rehydrated with the supplied wash buffer (20 mM Tris-HCl (pH 7.6), 137 mM NaCl, 0.01% (w/v) BSA, 0.05% (v/v) Tween[®] 20) and biotinylated oligonucleotide was immobilized onto the wells. The excess of oligonucleotide was then

washed off, and the enzyme assay carried out in the wells. The final reaction volume of 30 μ L in buffer (40 mM HEPES KOH (pH 7.6), 100 mM potassium glutamate, 10 mM magnesium acetate, 10 mM DTT, 1 mM ATP, 0.05 mg/mL albumin) contained 1.5 U of topoisomerase IV from *E. coli* or *S. aureus*, 0.75 μ g of supercoiled pNO1 plasmid, and 3 μ L of inhibitors solution in 10% DMSO and 0.008% Tween 20. Reactions were incubated for 30 min at 37 °C, and after addition of the TF buffer (50 mM NaOAc pH 5.0, 50 mM NaCl and 50 mM MgCl₂), which terminated the enzymatic reaction, for another 30 min at room temperature to allow triplex formation (biotin–oligonucleotide–plasmid). The unbound plasmid was then washed off using TF buffer and the solution of SybrGOLD stain in T10 buffer (10 mM Tris-HCl pH 8.0 and 1 mM EDTA) was added. After mixing, fluorescence (excitation, 485 nm; emission, 535 nm) was read using a BioTek's Synergy H4 microplate reader. Preliminary screening was performed at inhibitor concentrations of 100 μ M and 10 μ M. For most potent compounds IC₅₀ was determined with 7 concentrations of the inhibitors. IC₅₀ values were calculated using GraphPad Prism software and represent the concentration of inhibitor where the residual activity of the enzyme is 50% in three independent measurements; the final result is given as their average value. Novobiocin (IC₅₀ = 11 μ M (lit. 10 μ M [45]) for *E. coli* topoisomerase IV and IC₅₀ = 27 μ M (lit. 20 μ M [45]) for *S. aureus* topoisomerase IV) was used as a positive control.

4.6 Determination of Antibacterial Activity. Antimicrobial assays were performed by the broth microdilution method following the guidelines of the Clinical and Laboratory Standards Institute (CLSI; Methods for dilution antimicrobial susceptibility tests for bacteria that grow aerobically, Approved standards – Ninth Edition; M07-A9, Vol.32 No.2). The following CLSI recommended quality control strains for susceptibility testing were used in the antibacterial assays: *Enterococcus faecalis* (Gram positive, ATCC 29212), *Staphylococcus aureus* (Gram positive, ATCC 25923), *Escherichia coli* (Gram negative, ATCC 25922) and

Pseudomonas aeruginosa (Gram negative, ATCC 27853). Primary screening of compounds against the ATCC strains was initially carried out at a final concentration of 50 μ M ($n = 3$). Compound **35** that showed >80% inhibition against *E. faecalis* in the primary screen was tested further at 10 different concentrations to confirm its activity and to determine the MIC₉₀ concentration (lowest concentration inhibiting the growth by >90%). Ciprofloxacin (ICN Biomedicals Inc., USA) was used as positive control on every assay plate at MIC₉₀ concentration.

4.7 Molecular Modeling.

Ligand and Protein Preparation. Three-dimensional models of designed compounds were built in ChemBio3D Ultra 13.0 [46] Their geometries were optimized using MMFF94 [47] force field and partial atomic charges were added. Energy was minimized until the gradient value was smaller than 0.001 kcal/(mol Å). The optimized structure was further refined with GAMESS interface in ChemBio3D Ultra 13.0 using the semiempirical PM3 method, QA optimization algorithm and Gasteiger Hückel charges for all atoms for 100 steps [47]. Molecular docking calculations were performed using FlexX [48,49], as available in LeadIT [37], running on four octal core AMD Opteron CPU processors, 16 GB RAM, two 750 GB hard drives, running 64-bit Scientific Linux 6.0. Receptor was prepared in a LeadIT graphical user interface using the Receptor wizard. Amino acid residues within a radius of 7 Å around the ligand from the X-ray structure (PDB entry: 4DUH [39]) were defined as the binding site. Hydrogen atoms were added to the binding site residues and correct tautomers and protonation states were assigned. Water molecules, except HOH614, and the ligand were deleted from the crystal structure.

Ligand Docking. The FlexX molecular docking program, as available in LeadIT [37], was used for ligand docking. A hybrid algorithm (enthalpy and entropy driven ligand binding) was

used to place the 'base fragment'. The maximum number of solutions per iteration and the maximum number of solutions per fragmentation parameter values were increased to 1000, while other parameters were set at their default values.

Proposed binding modes and scoring function scores of the top five highest scored docking poses per ligand were evaluated and the highest ranked binding pose was used for graphical representation in PyMOL 3.1 [38].

Supporting Information. ^1H and ^{13}C NMR spectra of representative compounds. This material is available free of charge via the Internet.

Acknowledgments

This work was supported by the Slovenian Research Agency (Grant No. P1-0208), by the Academy of Finland (Grant No. 277001 and 284477) and by the EU FP7 Project MAREX: Exploring Marine Resources for Bioactive Compounds: from Discovery to Sustainable Production and Industrial Applications (Project No. FP7-KBBE-2009-3-245137). The authors thank Dr. Dušan Žigon (Mass Spectrometry Center, Jožef Stefan Institute, Ljubljana, Slovenia) for recording mass spectra. The authors thank Prof. Roger Pain for proofreading the manuscript.

Conflict of interest. The authors declare that there is no conflict of interest.

5. REFERENCES AND NOTES

[1] Boucher, H. W.; Talbot, G. H.; Bradley, J. S.; Edwards, J. E.; Gilbert, D.; Rice, L. B.; Scheld, M.; Spellberg, B.; Bartlett, J. Bad bugs, no drugs: no ESKAPE! An update from the Infectious Diseases Society of America. *Clin. Infect. Dis.* **2009**, *48*, 1-12.

- [2] Uria-Nickelsen, M.; Blodgett, A.; Kamp, H.; Eakin, A.; Sherer, B.; Green, O. Novel DNA gyrase inhibitors: microbiological characterisation of pyrrolamides. *Int. J. Antimicrob. Agents* **2013**, *41*, 28-35.
- [3] Eakin, A. E.; Green, O.; Hales, N.; Walkup, G. K.; Bist, S.; Singh, A.; Mullen, G.; Bryant, J.; Embrey, K.; Gao, N.; Breeze, A.; Timms, D.; Andrews, B.; Uria-Nickelsen, M.; Demeritt, J.; Loch III, J. T.; Hull, K.; Blodgett, A.; Illingworth, R. N.; Prince, B.; Boriack-Sjodin, P. A.; Hauck, S.; MacPherson, L. J.; Ni, H.; Sherer, B. Pyrrolamide DNA gyrase inhibitors: fragment-based nuclear magnetic resonance screening to identify antibacterial agents. *Antimicrob. Agents Chemotherap.* **2012**, *56*, 1240-1246.
- [4] Manchester, J. I.; Dussault, D. D.; Rose, J. A.; Boriack-Sjodin, P. A.; Uria-Nickelsen, M.; Ioannidis, G.; Bist, S.; Fleming, P.; Hull, K. G. Discovery of a novel azaindole class of antibacterial agents targeting the ATPase domains of DNA gyrase and topoisomerase IV. *Bioorg. Med. Chem. Lett.* **2012**, *22*, 5150-5156.
- [5] Sissi, C.; Palumbo, M. In front of and behind the replication fork: bacterial type IIA topoisomerases. *Cell Mol. Life Sci.* **2010**, *67*, 2001-2024.
- [6] Mayer, C.; Janin, Y. L. Non-quinolone inhibitors of bacterial type IIA topoisomerases: a feat of bioisosterism. *Chem. Rev.* **2014**, *114*, 2313-2342.
- [7] Bisacchi, G. S.; Manchester, J. I. A new-class antibacterial—almost. Lessons in drug discovery and development: A critical analysis of more than 50 years of effort toward ATPase inhibitors of DNA gyrase and topoisomerase IV. *ACS Infect. Dis.* **2015**, *1*, 4-41.
- [8] Tomašič, T.; Mašič, L. P. Prospects for developing new antibacterials targeting bacterial type IIA topoisomerases. *Curr. Top. Med. Chem.* **2014**, *14*, 130-151.
- [9] Sherer, B. A.; Hull, K.; Green, O.; Basarab, G.; Hauck, S.; Hill, P.; Loch, J. T., 3rd; Mullen, G.; Bist, S.; Bryant, J.; Boriack-Sjodin, A.; Read, J.; DeGrace, N.; Uria-Nickelsen,

M.; Illingworth, R. N.; Eakin, A. E. Pyrrolamide DNA gyrase inhibitors: optimization of antibacterial activity and efficacy. *Bioorg. Med. Chem. Lett.* **2011**, *21*, 7416-7420.

[10] Maxwell, A.; Lawson, D. M. The ATP-binding site of type II topoisomerases as a target for antibacterial drugs. *Curr. Top. Med. Chem.* **2003**, *3*, 283-303.

[11] Trzoss, M.; Bensen, D. C.; Li, X.; Chen, Z.; Lam, T.; Zhang, J.; Creighton, C. J.; Cunningham, M. L.; Kwan, B.; Stidham, M.; Nelson, K.; Brown-Driver, V.; Castellano, A.; Shaw, K. J.; Lightstone, F. C.; Wong, S. E.; Nguyen, T. B.; Finn, J.; Tari, L. W. Pyrrolopyrimidine inhibitors of DNA gyrase B (GyrB) and topoisomerase IV (ParE), Part II: development of inhibitors with broad spectrum, Gram-negative antibacterial activity. *Bioorg. Med. Chem. Lett.* **2013**, *23*, 1537-1543.

[12] East, S. P.; White, C. B.; Barker, O.; Barker, S.; Bennett, J.; Brown, D.; Boyd, E. A.; Brennan, C.; Chowdhury, C.; Collins, I.; Convers-Reignier, E.; Dymock, B. W.; Fletcher, R.; Haydon, D. J.; Gardiner, M.; Hatcher, S.; Ingram, P.; Lancett, P.; Mortenson, P.; Papadopoulos, K.; Smee, C.; Thomaides-Brears, H. B.; Tye, H.; Workman, J.; Czaplewski, L. G. DNA gyrase (GyrB)/topoisomerase IV (ParE) inhibitors: synthesis and antibacterial activity. *Bioorg. Med. Chem. Lett.* **2009**, *19*, 894-899.

[13] Tari, L. W.; Trzoss, M.; Bensen, D. C.; Li, X.; Chen, Z.; Lam, T.; Zhang, J.; Creighton, C. J.; Cunningham, M. L.; Kwan, B.; Stidham, M.; Shaw, K. J.; Lightstone, F. C.; Wong, S. E.; Nguyen, T. B.; Nix, J.; Finn, J. Pyrrolopyrimidine inhibitors of DNA gyrase B (GyrB) and topoisomerase IV (ParE). Part I: Structure guided discovery and optimization of dual targeting agents with potent, broad-spectrum enzymatic activity. *Bioorg. Med. Chem. Lett.* **2013**, *23*, 1529-1536.

[14] Goetschi, E.; Angehrn, P.; Gmuender, H.; Hebeisen, P.; Link, H.; Masciadri, R.; Nielsen, J. Cyclothialidine and its congeners: a new class of DNA gyrase inhibitors. *Pharmacol. Ther.* **1993**, *60*, 367-380.

- [15] Angehrn, P.; Buchmann, S.; Funk, C.; Goetschi, E.; Gmuender, H.; Hebeisen, P.; Kostrewa, D.; Link, H.; Luebbers, T.; Masciadri, R.; Nielsen, J.; Reindl, P.; Ricklin, F.; Schmitt-Hoffmann, A.; Theil, F.-P. New antibacterial agents derived from DNA gyrase inhibitor cyclothialidine. *J. Med. Chem.* **2004**, *47*, 1487-1513.
- [16] Angehrn, P.; Goetschi, E.; Gmuender, H.; Hebeisen, P.; Hennig, M.; Kuhn, B.; Luebbers, T.; Reindl, P.; Ricklin, F.; Schmitt-Hoffmann, A. A new DNA gyrase inhibitor subclass of the cyclothialidine family based on a bicyclic dilactam-lactone scaffold. Synthesis and antibacterial properties. *J. Med. Chem.* **2011**, *54*, 2207-2224.
- [17] Wigley, D. B.; Davies, G. J.; Dodson, E. J.; Maxwell, A.; Dodson, G. Crystal structure of an N-terminal fragment of the DNA gyrase B protein. *Nature* **1991**, *351*, 624-629.
- [18] Lewis, J. R.; Singh, O. M. P.; Smith, C. V.; Skarzynsky, T.; Maxwell, A.; Wonacott, A. J.; Wigley, D. B. The nature of inhibition of DNA gyrase by the coumarins and the cyclothialidines revealed by X-ray crystallography. *EMBO J.* **1996**, *15*, 1412-1420.
- [19] Tsai. The high-resolution crystal structure of a 24-kDa gyrase B fragment from *Escherichia Coli* complexed with one of the most potent coumarin inhibitors, clorobiocin. *Proteins* **1997**, *28*, 41-52.
- [20] Musicki, B.; Periers, A.; Laurin, P.; Ferroud, D.; Benedetti, Y.; Lachaud, S.; Chatreaux, F.; Haesslein, J.; Iltis, A.; Pierre, C.; Khider, J.; Tessot, N.; Airault, M.; Demasse, J.; Dupuis-Hamelin, C.; Lassaigne, P.; Bonnefoy, A.; Vicat, P.; Klich, M. Improved antibacterial activities of coumarin antibiotics bearing 5',5'-dialkylnoviose: biological activity of RU79115. *Bioorg. Med. Chem. Lett.* **2000**, *10*, 1695-1699.
- [21] Poyser, J. P.; Telford, B.; Timms, D.; Block, M. H.; Hales, N. J. Triazine derivatives and their use as antibacterials. WO Patent 99/01442, 1999.
- [22] Tanitame, A.; Oyamada, Y.; Ofuji, K.; Kyoya, Y.; Suzuki, K.; Ito, H.; Terauchi, H.; Kawasaki, M.; Nagai, K.; Wachi, M.; Yamagishi, J. Design, synthesis and structure-activity

relationship studies of novel indazole analogues as DNA gyrase inhibitors with Gram-positive antibacterial activity. *Bioorg. Med. Chem. Lett.* **2004**, *14*, 2857-2862.

[23] Zhana, J.; Cross, J.; Yang, Q.; Mesleh, M.; Romero, J.; Wang, B.; Bevan, D.; Hall, K.; Epie, J.; Moy, T.; Daniel, A.; Shotwell, J.; Chamberlain, B.; Carter, N.; Ryan, D.; Metcalf, C.; Silverman, J.; Nguyen, K.; Lippa, B.; Dolle, R. The discovery of pyrazolopyridones as a novel class of gyrase B inhibitors through fragment- and structure-based drug discovery: SAR studies and antibacterial activity. *53rd Interscience Conference on Antimicrobial Agents and Chemotherapy*; Denver, CO, **2013**; abstract F-1224.

[24] Basarab, G. S.; Manchester, J. I.; Bist, S.; Boriack-Sjodin, P. A.; Dangel, B.; Illingworth, R.; Sherer, B. A.; Sriram, S.; Uria-Nickelsen, M.; Eakin, A. E. Fragment-to-hit-to-lead discovery of a novel pyridylurea scaffold of ATP competitive dual targeting type II topoisomerase inhibiting antibacterial agents. *J. Med. Chem.* **2013**, *56*, 8712-8735.

[25] Basarab, G. S.; Hill, P. J.; Garner, C. E.; Hull, K.; Green, O.; Sherer, B. A.; Dangel, P. B.; Manchester, J. I.; Bist, S.; Hauck, S.; Zhou, F.; Uria-Nickelsen, M.; Illingworth, R.; Alm, R.; Rooney, M.; Eakin, A. E. Optimization of pyrrolamide topoisomerase II inhibitors toward identification of an antibacterial clinical candidate (AZD5099). *J. Med. Chem.* **2014**, *57*, 6060-6082.

[26] Tari, L. W.; Li, X.; Trzoss, M.; Bensen, D. C.; Chen, Z.; Lam, T.; Zhang, J.; Lee, S. J.; Hough, G.; Phillipson, D.; Akers-Rodriguez, S.; Cunningham, M. L.; Kwan, B. P.; Nelson, K. J.; Castellano, A.; Locke, J. B.; Brown-Driver, V.; Murphy, T. M.; Ong, V. S.; Pillar, C. M.; Shinabarger, D. L.; Nix, J.; Lightstone, F. C.; Wong, S. E.; Nguyen, T. B.; Shaw, K. J.; Finn, J. Tricyclic GyrB/ParE (TriBE) inhibitors: a new class of broad-spectrum dual-targeting antibacterial agents. *PLoS One* **2013**, *8*, e84409.

[27] Walsh, C. T.; Wencewicz, T. A. Prospects for new antibiotics: a molecule-centered perspective. *J. Antibiotics* **2014**, *67*, 7-22.

- [28] Boström J.; Hogner, A.; Llinás, A.; Wellner, E.; Plowright, A. T. Oxadiazoles in medicinal chemistry. *J. Med. Chem.* **2012**, *55*, 1817-1830.
- [29] Jakopin, Ž.; Sollner Dolenc, M. Recent advances in the synthesis of 1,2,4- and 1,3,4-oxadiazoles. *Curr. Org. Chem.* **2008**, *12*, 850-898.
- [30] Jakopin, Ž.; Roškar, R.; Sollner Dolenc, M. Synthesis of 3,5-disubstituted 1,2,4-oxadiazoles as peptidomimetic building blocks. *Tetrahedron Lett.* **2007**, *48*, 1465-1468.
- [31] Lu, J.; Patel, S.; Sharma, N.; Soisson, S. M.; Kishii, R.; Takei, M.; Fukuda, Y.; Lumb, K. J.; Singh, S. B. Structures of kbidelomycin bound to *Staphylococcus aureus* GyrB and ParE showed a novel U-shaped binding mode. *ACS Chem. Biol.* **2014**, *9*, 2023-2031.
- [32] Tomašič, T.; Katsamakas, S.; Hodnik, Ž.; Ilaš, J.; Brvar, M.; Šolmajer, T.; Montalvao, S.; Tammela, P.; Banjanac, M.; Ergović, G.; Anderluh, M.; Mašič, L.P.; Kikelj, D., Discovery of 4,5,6,7-Tetrahydrobenzo[1,2-*d*]thiazoles as novel DNA gyrase inhibitors targeting the ATP-binding site. *J. Med. Chem.* **2015**, *58*, 5501-5521.
- [33] Zidar, N.; Macut, H.; Tomašič, T.; Brvar, M.; Montalvao, S.; Tammela, P.; Šolmajer, T.; Mašič, L.P.; Ilaš, J.; Kikelj, D., *N*-Phenyl-4,5-dibromopyrrolamides and *N*-Phenylindolamides as ATP competitive DNA gyrase B inhibitors: Design, synthesis and evaluation. *J. Med. Chem.* **2015**, *58*, 6179-6194.
- [34] Gjorgjieva, M.; Tomašič, T.; Barančokova, M.; Katsamakas, S.; Ilaš, J.; Tammela, P.; Mašič, L.P.; Kikelj, D., Discovery of benzothiazole scaffold-based DNA gyrase B inhibitors. *J. Med. Chem.* **2016**, accepted manuscript, doi: 10.1021/acs.jmedchem.6b00864.
- [35] Zidar, N.; Tomašič, T.; Macut, H.; Sirc, A.; Brvar, M.; Montalvao, S.; Tammela, P.; Ilaš, J.; Kikelj, D., New *N*-Phenyl-4,5-dibromopyrrolamides and *N*-Phenylindolamides as ATPase inhibitors of DNA gyrase. *Eur. J. Med. Chem.* **2016**, *117*, 197-211.

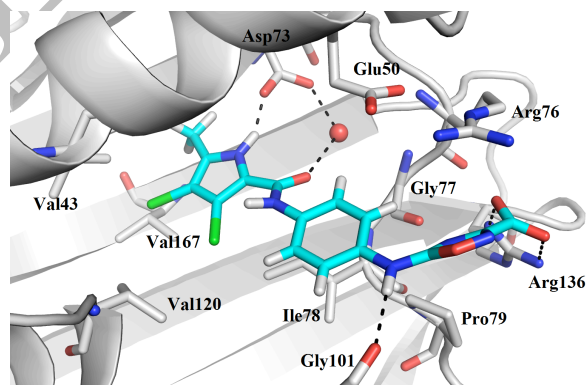
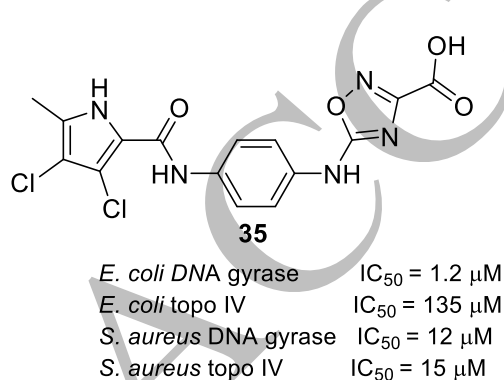
- [36] Jeankumar, V. U.; Reshma, R. S.; Vats, R.; Janupally, R.; Saxena, S.; Yogeeswari, P.; Sriram, D. Engineering another class of anti-tubercular lead: Hit to lead optimization of an intriguing class of gyrase ATPase inhibitors. *Eur. J. Med. Chem.* **2016**, *122*, 216-231.
- [37] BioSolve IT (GmbH), LeadIT version 2.1.3.
- [38] PyMOL, Delano Scientific LLC, San Francisco, CA, <http://pymol.sourceforge.net>.
- [39] Brvar, M.; Perdih, A.; Renko, M.; Anderluh, G.; Turk, D.; Šolmajer, T. Structure-based discovery of substituted 4,5'-bithiazoles as novel DNA gyrase inhibitors. *J. Med. Chem.* **2012**, *55*, 6413-6426.
- [40] Huguet, F.; Melet, A.; Alves de Sousa, R.; Lieutaud, A.; Chevalier, J.; Maigre, L.; Deschamps, P.; Tomas, A.; Leulliot, N.; Pages, J. M.; Artaud, I. Hydroxamic acids as potent inhibitors of Fe(II) and Mn(II) *E. coli* methionine aminopeptidase: biological activities and X-ray structures of oxazole hydroxamate-EcMetAP-Mn complexes. *ChemMedChem* **2012**, *7*, 1020-1030.
- [41] Urbanek, R.; Brown, D.; Steelman, G.; Blackwell, W.; Wesolowski, S.; Wang, X. **2007** Compounds. PCT Int. Appl. WO 2007078251.
- [42] Jakopin, Ž. Orthogonally Protected Oxadiazole-Based Building Blocks: Synthesis and Characterization. *Curr. Org. Synth.* **2015**, *13*, 126-131.
- [43] Ross, J. W.; Verge, J. P.; Williamson, W. R. N. Acylamino-1,2,4-oxadiazole or thiadiazole derivatives as anti-hypersensitivity agents. US Patent US4163048.
- [44] Shaw, J. T.; Coffindaffer, T. W.; Stimmel, J. B.; Lindley, P. M. Fused-*s*-triazino heterocycles IX. 1,3,4,6,9b-pentaazaphenalenenes and 1,3,6,9b-tetraazaphenalenenes: Amino and alkoxy derivatives. *J. Het. Chem.* **1982**, *19*, 357-361.
- [45] Alt, S.; Mitchenall, L. A.; Maxwell, A.; Heide, L. Inhibition of DNA gyrase and DNA topoisomerase IV of *Staphylococcus aureus* and *Escherichia coli* by aminocoumarin antibiotics. *J. Antimicrob. Chemother.* **2011**, *66*, 2061-2069.

- [46] GAMESS interface, ChemBio3D Ultra 13.0, ChemBioOffice Ultra 13.0, CambridgeSoft.
- [47] Halgren, T. A. Merck molecular force field .1. Basis, form, scope, parameterization, and performance of MMFF94. *J. Comput. Chem.* **1996**, *17*, 490-519.
- [48] Rarey, M.; Kramer, B.; Lengauer, T.; Klebe, G. A fast flexible docking method using an incremental construction algorithm. *J. Mol. Biol.* **1996**, *261*, 470-489.
- [49] Rarey, M.; Wefing, S.; Lengauer, T. Placement of medium-sized molecular fragments into active sites of proteins. *J. Comput. Aid. Mol. Des.* **1996**, *10*, 41-54.

RESEARCH HIGHLIGHTS

- Structurally novel inhibitors of DNA gyrase were revealed by computer aided design
- Oxadiazoles identified as balanced inhibitors of DNA gyrase and topoisomerase IV
- Structural requirements for DNA gyrase and topo IV inhibition were identified

GRAPHICAL ABSTRACT



FIGURES

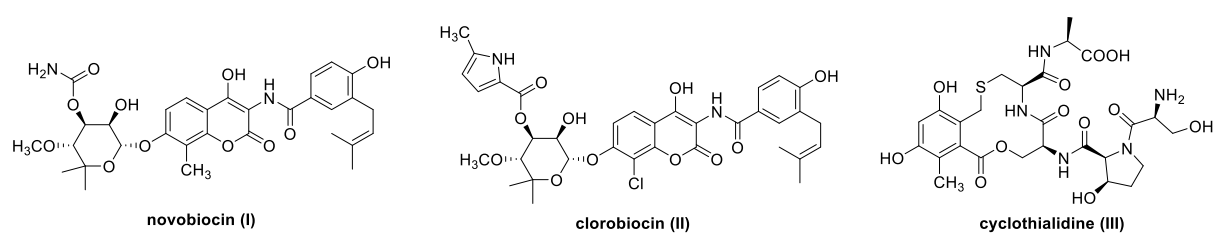


Figure 1. Naturally occurring DNA gyrase inhibitors

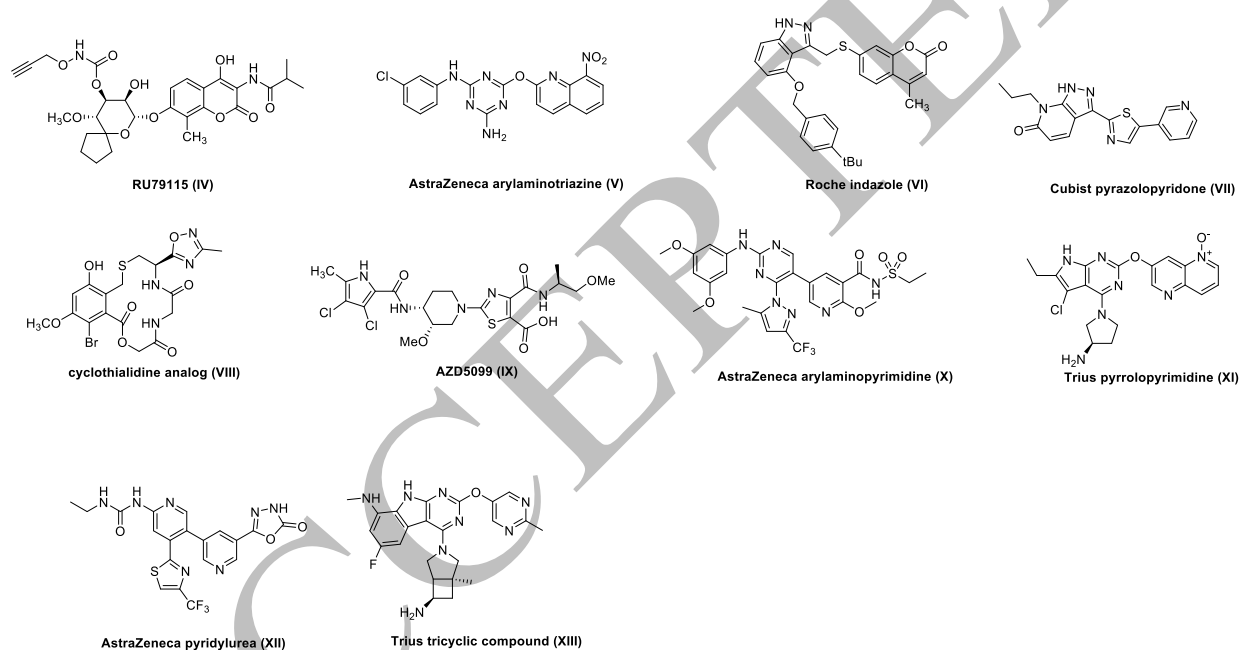


Figure 2. Representative examples of synthetic DNA gyrase and/or topoisomerase IV inhibitors.

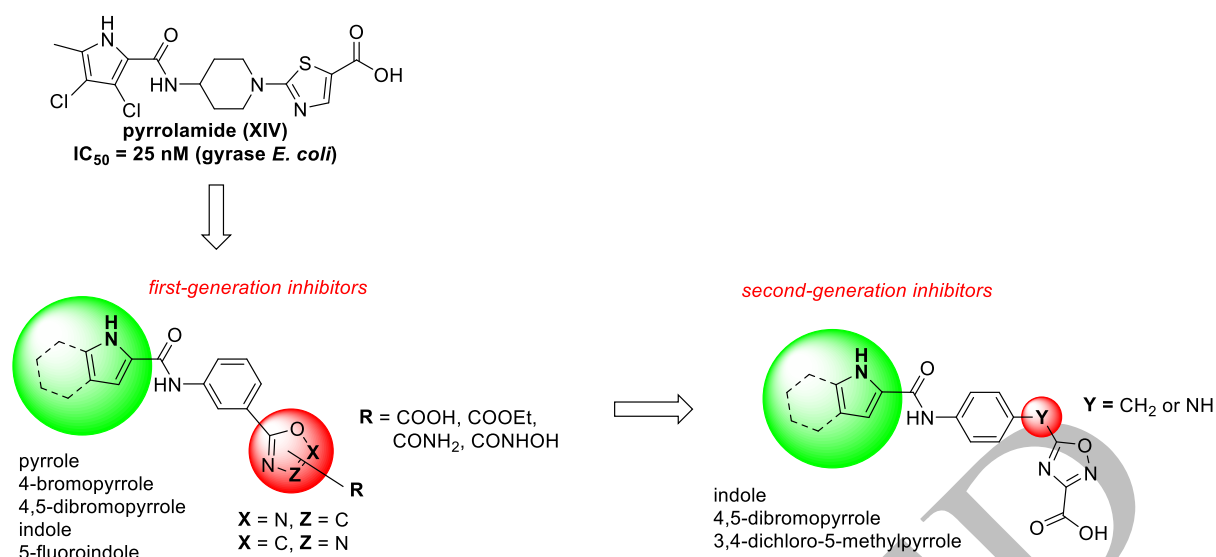


Figure 3. Design of oxadiazole-based DNA gyrase inhibitors.

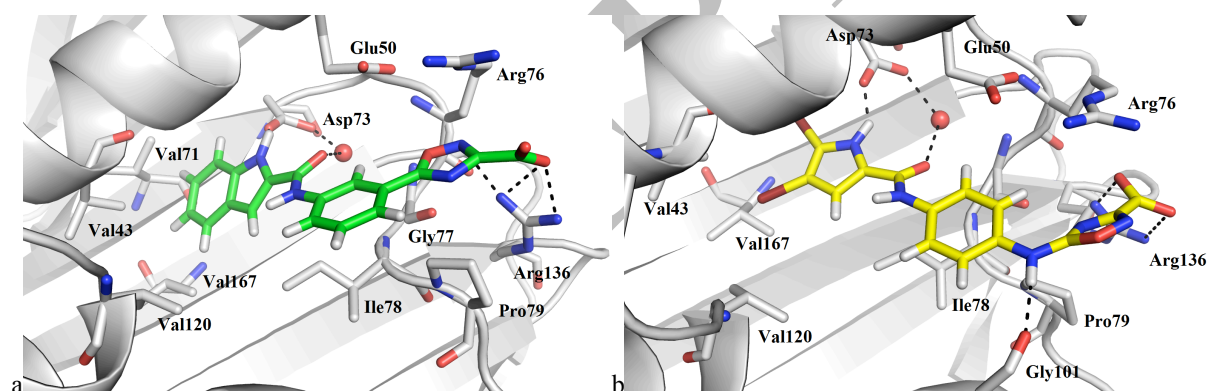


Figure 4. The binding mode of inhibitors a) **19** (in green sticks) and b) **34** (in yellow sticks) in the ATP-binding site of *E. coli* DNA gyrase B (PDB code: 4DUH) as predicted by docking with LeadIT [37]. The ligand and neighboring protein side chains are colored according to the chemical atom type (C_{19} in green, C_{34} in yellow, C_{GyrB} in gray, N in blue, O in red, and Br in brown). Hydrogen bonds are indicated by black dotted lines. Figure was prepared by PyMOL [38].